

Manuscript prepared for Atmos. Chem. Phys.
with version 2015/11/06 7.99 Copernicus papers of the L^AT_EX class copernicus.cls.
Date: 16 July 2016

Scalar turbulent behavior in the roughness sublayer of an Amazonian forest. Answer to Reviewers

Zahn, Dias et al.

Correspondence to: Nelson L. Dias (nldias@ufpr.br)

1 Answer to Editor's Letter:

We thank the Editor and the Reviewers for the comments. We answer the all remaining comments and suggestions below.

Reviewer(s)' Comments to Author:

5 Reviewer: 1

Comments to the Author

The study by Zahn et al. focuses on the analysis of the atmospheric boundary layer structure in the roughness sublayer of an Amazonian forest. Measurements of atmospheric turbulence made at several levels of the 82-m tower are used to study turbulent fluxes, scaling laws for turbulent mixing, and dissipation rates of various scalars (temperature, water vapour, and carbon dioxide). In this paper, the authors extensive debate on the breakdown of Monin-Obukov similarity theory (MOST) in the roughness sublayer under unstable conditions. I understand that the authors have done an extensive data analysis and reported among other things the importance of the solar zenith angle for similarity of scalars. In general, the authors have set out the problem and carefully worked out what needs to be done to address several issues. The paper is original, makes a significant contribution and is well written. I recommend acceptance of the paper for publication in the ACP with minor revisions, not so much in terms of redoing the analysis, but rather providing perspective on important questions and difficulties.

We thank the reviewer for all his comments. We give a detailed answer to the specific below

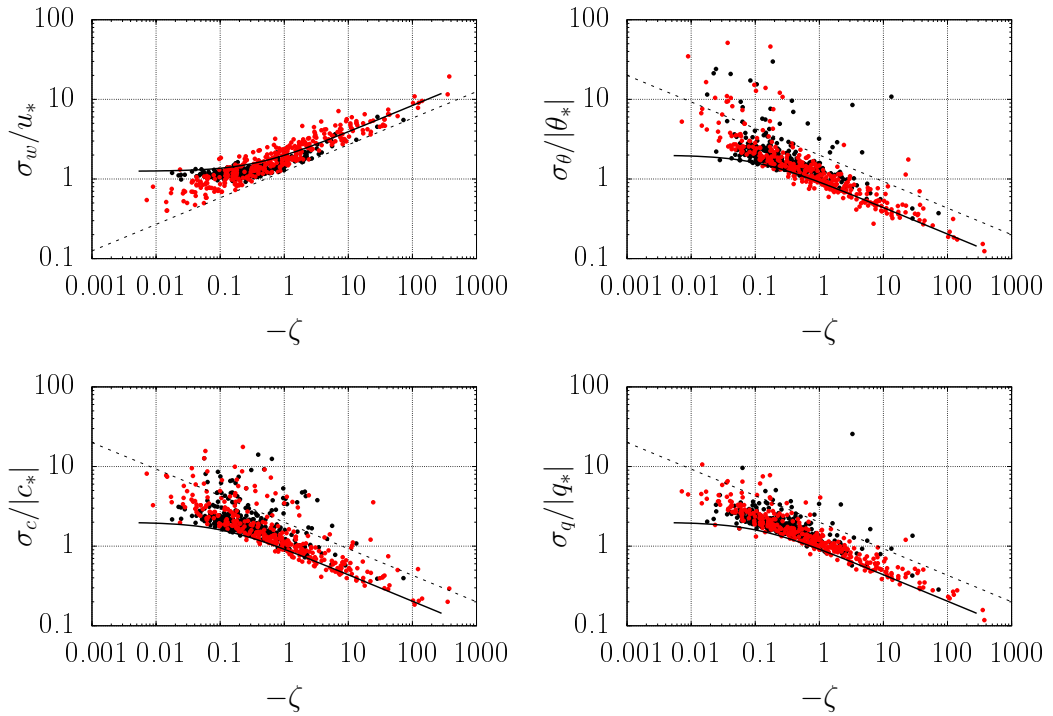
20 1. My main concern is associated with self-correlation (also referred to as artificial or spurious correlation), which occurs in some plots because of the shared variables. Awareness regarding the self-correlation has been increasing in the past several years (e.g., Andreas and Hicks, 2002; Klipp and Mahrt, 2004; Baas et al., 2006; Grachev et al. 2007 and papers surveyed therein). Authors say nothing about this problem. However, some of the results (e.g., plots of

25 various similarity functions in Figures 4-7) may be suffered by self-correlation because have built-in correlation that is not associated with real physics. For example, increasing σ_w/u_* with increasing $-z/L$ (1/3 power law) is likely associated with self-correlation because same variables (friction velocity) appear in two quantities between which a functional relationship is sought. I would like to see here some discussion on this point.

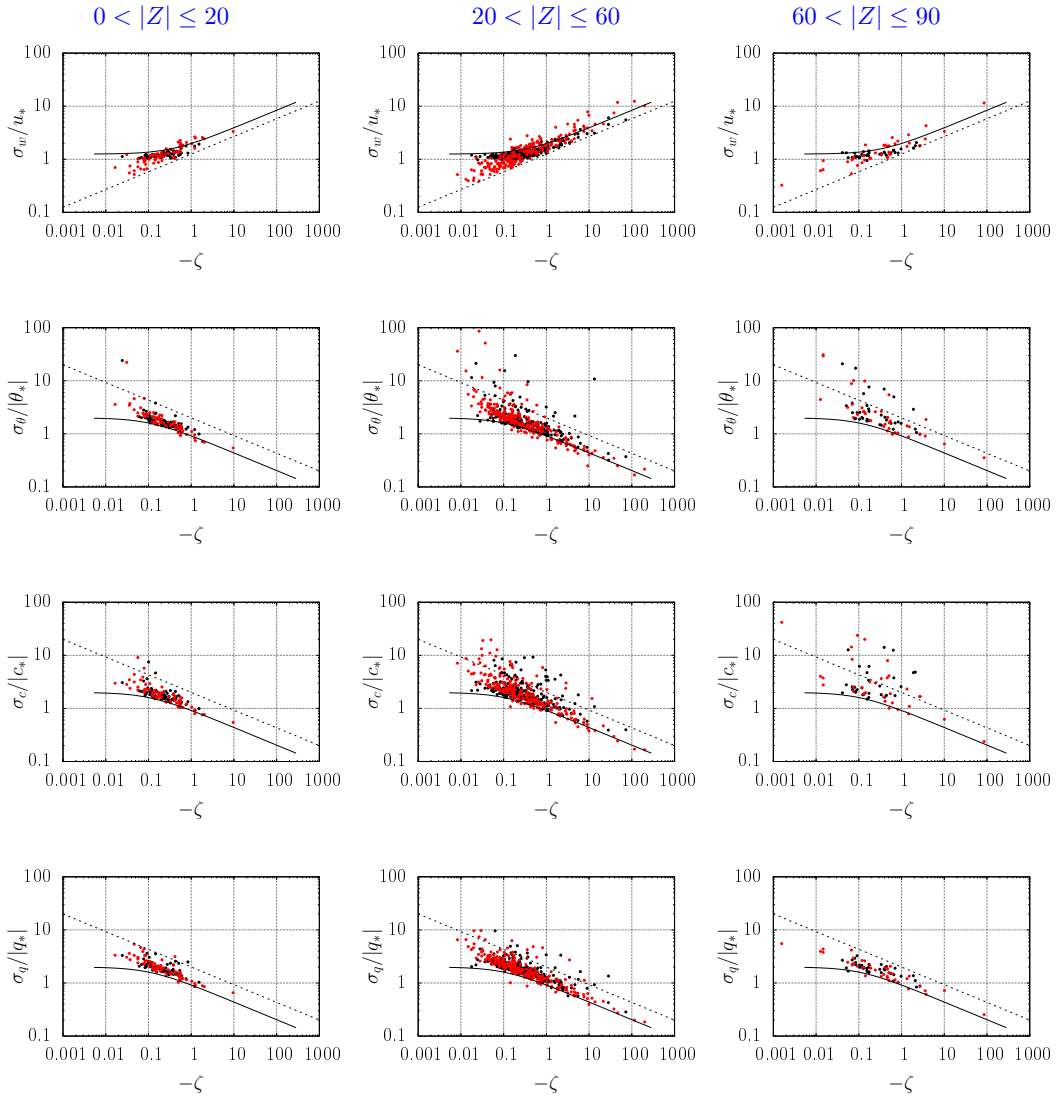
30 We thank the reviewer for bringing up the issue of self-correlation, which is something we had not addressed in the previous version. The issue is complex, and undoubtedly still to some degree controversial since, as acknowledged from the start, the possibility that self-correlation contaminate data analysis does not by itself contradict the general validity of similarity theories (see, for example Hicks, 1981; Johansson et al., 2002). A very effective way to test the 35 extent to which self-correlation contaminates the analysis is still contained in the suggestion by Andreas and Hicks (2002) of randomizing the data set. Examples of application of this “self-correlation test” for the ϕ ’s can be found in von Randow et al. (2006) and Cava et al. (2008).

40 Following (Cava et al., 2008), our original plots were compared with the plots produced with randomised u_* (we retained the same scalar variances and covariances). The results can be seen in the figure below, which depicts the original plots of Figure 4 in the manuscript against the same data randomized (in red), where the dashed lines show a $-1/3$ power law. Our results are similar to Cava et al. (2008)’s results: although the randomised data follows 45 the $-1/3$ power law, it erroneously follows this tendency even at near-neutral regime, where the original data follows the predicted similarity functions. In this case, as stated by Cava et al. (2008), the correlations are not “spurious” in the near-neutral regimes.

50 We also calculated the scalar fluxes for fairly to highly unstable conditions ($-\zeta > 0.2$) using the flux-variance method, and compared them with the measured fluxes. We obtained high correlations (in fact, higher than those reported by Cava et al. (2008)). As these authors comment, these fluxes are calculated without knowledge of u_* , and the success of the method under these more unstable conditions gives independent confirmation that spurious correlation is not contaminating our analyses.



Next, the same results are displayed for each zenith angle range.



55

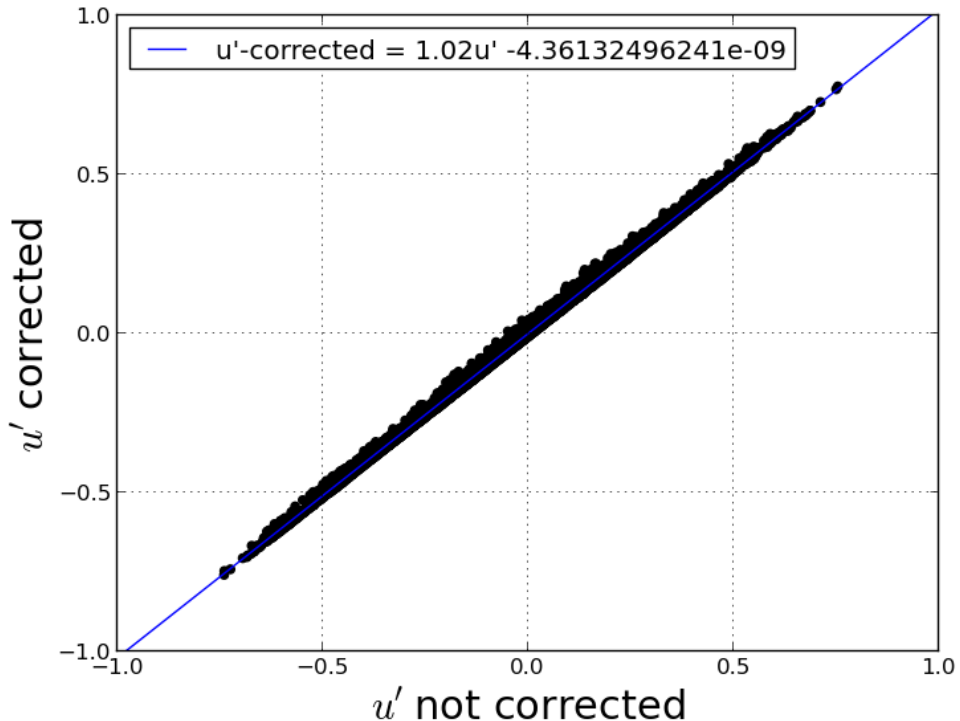
For completeness, we do discuss self-correlation in lines 304–317 of the current version of the manuscript.

60 2. Section 2.1 (page 4, line 111). Use of a CSAT3 sonic anemometer now requires flow distortion correction. The recent controversy concerning the underestimation of vertical wind speed by non-orthogonal sonic anemometers has largely been resolved (see papers by Horst et al. (2015, BLM - reference is below) and B51K-01 (Frank et al.) and B51K-02 (Horst et al.) at the 2014 American Geophysical Union Fall meeting). I recommend the authors download Tom Horst's AGU talk and BLM paper, available at his website www.eol.ucar.edu/homes/horst/ However, this likely would not affect the general results of this study.

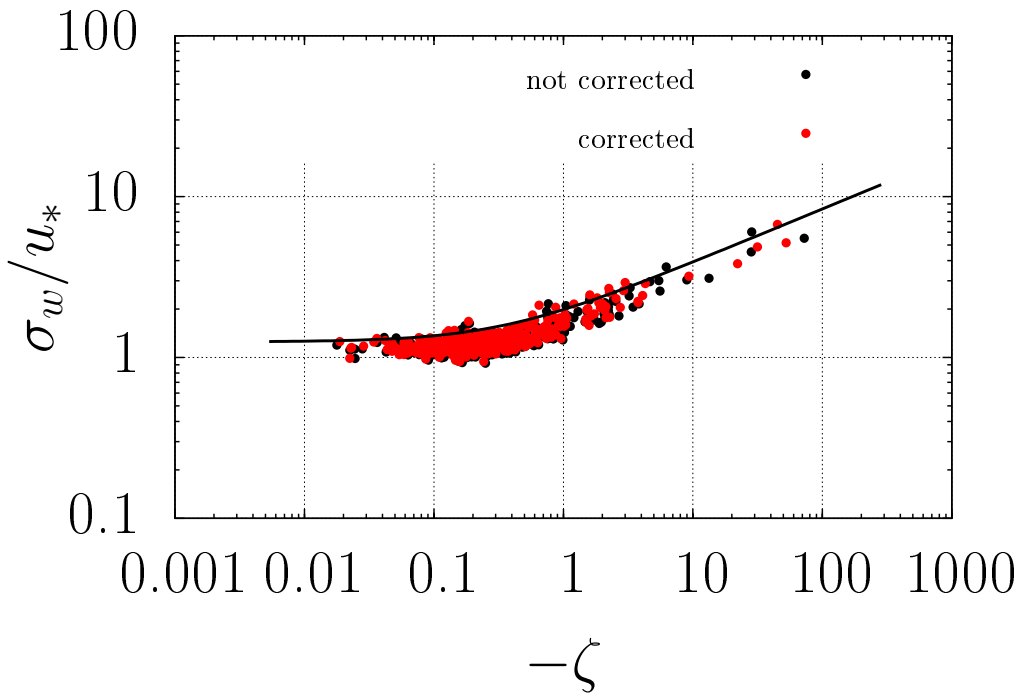
65 We thank the reviewer for the helpful suggestion. In this case, as the reviewer correctly predicted, flow distortion corrections do not change appreciably any of our results. To show this,

we did apply the corrections suggested by Horst et al. (2015), to the CSAT-3 data. As an example, the figure below compares the u' fluctuations before and after the corrections. As can be seen, the differences are only minor.

70



Next, we also checked the effects of flow distortion on some of our statistics (in this case, σ_w/u_*). The results with and without correction are shown in the figure below.



75

To summarize, after careful consideration, flow distortion corrections do not change our results appreciably. With this in mind, we chose not to apply them in the results shown in the paper. At any rate, we mention this issue explicitly in the paper now, in lines 132–137.

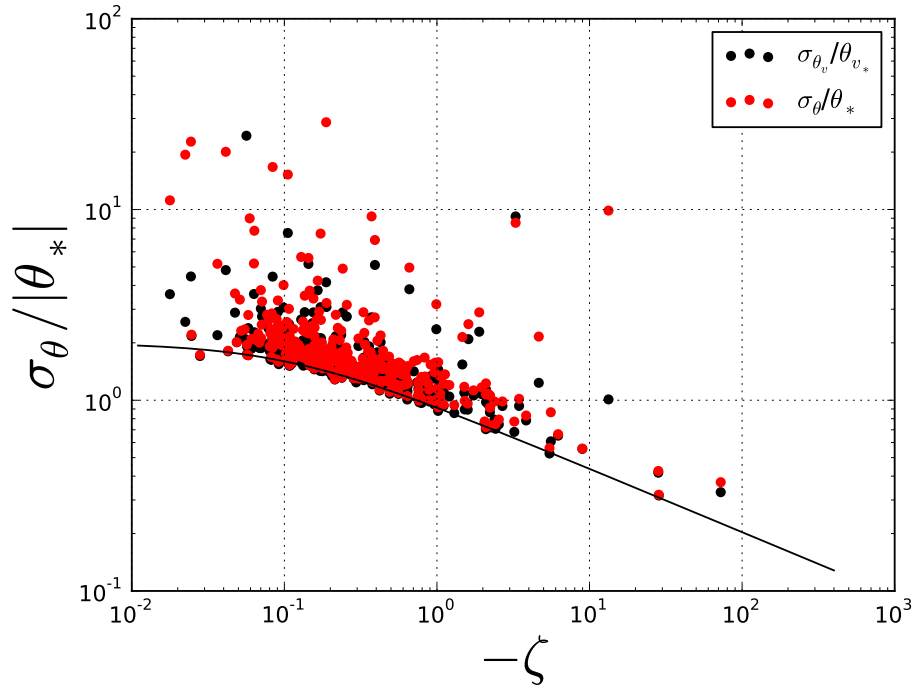
80 3. Since the sonic anemometer measures the so-called sonic virtual temperature (which is close to the virtual temperature) the moisture correction in the sonic anemometer signal is necessary to obtain the correct value of temperature itself and sensible heat flux (e.g. Kaimal and Finnigan, 1994). Authors reported the standard deviation of the temperature (Figures 4-6) and temperature spectra (Eq.6). To value the present results the authors should either show that the moisture corrections and their impact on the results are small, or (if otherwise) apply moisture corrections to the sonic temperature following Schotanus et al. (1983) based on the data collected by LI-7500.

85

90 We agree with the Reviewer. We note that the Schotanus et al. paper actually deals with corrections of the sonic temperature which are already incorporated into the outputs of both the CSAT3 and the Gill sonic anemometers according to the sonics' manuals. Regarding the data themselves, we have re-calculated all temperature, humidity and CO₂ data to derive good estimates of instantaneous thermodynamic temperature, specific humidity and CO₂ mass concentration. With these data, no further density corrections are needed, and the calculation of the

turbulence statistics presented in the paper are straightforward. Details about this procedure are now given in lines 124–131 of the current version of the manuscript.

We would also like to add that the actual changes in our former results are very small. As an example, we present a comparison for temperature σ_θ/θ_* statistics in the figure below: black means former results and red means corrected values.



4. Authors say nothing about the Webb correction (called WPL or Webb effect after the paper by Webb et al. [1980]). This correction must be taken into account when the turbulent fluxes of minor constituents such as carbon dioxide or, in some cases, water vapor are measured (Webb et al. 1980).

We agree. We have re-calculated all our data making the necessary corrections. This is already mentioned in the answer above. Again, the detailed descriptions and references now appear in lines 124–131 of the current version of the manuscript.

5. Section 2.2. Important discussion on the QC recommendations by Klipp and Mahrt (2004) and Sanz Rodrigo and Anderson (2013, their Table 1) have been missed. I think the authors should also include these papers in their discussion.

110 We thank the reviewer for suggesting the additional QC in the aforementioned papers. After
careful consideration, we came to the conclusion that these additional criteria cannot impact
our data: they deal with problems typical of stable conditions (mainly low-intensity or nonex-
isting turbulence), whereas we only worked with unstable data. Moreover, we did exclude
115 all runs whose two-minute standard deviations were less than a specified threshold (see lines
141–144 of the current version). Incidentally, our own current research on the topic has shown
that this test of ours is quite capable of identifying those low-intensity turbulence runs in sta-
ble conditions as well (Zahn et al., 2016). In view of that, we decided not to include these
references.

120 6. Page 6, line 164. Turbulence Kinetic Energy (TKE) has already been defined earlier in Section
3.1, line 136.

Done in line 196

7. Section 5.1. Define the scalar's turbulent scales a_* , c_* etc. Because, $c_* < 0$, the similarity
functions for 'c' in Figs. 4-6 should be defined as $\sigma_c/|c_*|$.

Done, in the new equation 9 and in lines 299–303

125 8. Literature, not mentioned in the manuscript

- (a) Andreas E.L, Hicks B.B. (2002) Comments on “Critical test of the validity of Monin-
Obukhov similarity during convective conditions.” *J. Atmos. Sci.* 59, 2605–2607.
- (b) Baas P., Steeneveld G.J., van de Wiel B.J.H., Holtslag A.A.M. (2006) Exploring Self-
Correlation in Flux-Gradient Relationships for Stably Stratified Conditions. *J. Atmos.*
Sci. 63(11), 3045–3054.
- (c) Grachev A.A., Andreas E.L, Fairall C.W., Guest P.S., Persson P.O.G. (2007) SHEBA
flux-profile relationships in the stable atmospheric boundary layer. *Boundary-Layer Me-
teorol.* 124(3), 315–333. DOI: 10.1007/s10546-007-9177-6
- (d) Horst T.W., Semmer S.R., Maclean G. (2015) Correction of a non-orthogonal, three-
component sonic anemometer for flow distortion by transducer shadowing. *Boundary-
Layer Meteorology*, 155(3): 371-395. DOI: 10.1007/s10546-015-0010-3
- (e) Klipp C.L., Mahrt L. (2004) Flux-Gradient Relationship, Self-correlation and Intermit-
tency in the Stable Boundary Layer. *Quart. J. Roy. Meteorol. Soc.* 130(601), 2087–2103.
- (f) Sanz Rodrigo J, Anderson P.S. (2013) Investigation of the stable atmospheric bound- ary
layer at Halley Antarctica. *Boundary-Layer Meteorol.* 148(3): 517-539. DOI: 10.1007/s10546-
013-9831-0
- (g) Schotanus P., Nieuwstadt F.T.M., De Bruin H.A.R. (1983) Temperature measurement
with a sonic anemometer and its application to heat and moisture fluxes. *Boundary-Layer
Meteorol.* 26(1): 81–93. DOI: 10.1007/BF00164332

145 (h) Webb E.K., Pearman G.I., Leuning R. (1980) Correction of flux measurements for density effects due to heat and water vapour transfer. *Q. J. R. Meteorol. Soc.* 106(447): 85–100. DOI: 10.1002/qj.49710644707

We thank the reviewer for the helpful suggestions. Many of the above works have now been incorporated into the references of the current version of the manuscript.

150 **Reviewer: 2**

Comments to the Author

The work reports new data in the roughness sublayer (RSL) above tall forests and features them in relation to Monin-Obukhov similarity theory (MOST). The main result of interest is that when the zenith angle is low, the radiation load appears to force higher spatial uniformity thereby making the 155 flow resemble surface layers (and hence follow MOST) - at least for heat and some of the biologically active scalars such as CO₂ and water vapor. All in all, the data are unique, and the analysis opens up new ways to thinking about the RSL. For these reasons, the paper may be published in *Atmos. Chem. Phys.* The comments below are mainly for the authors to consider - and should be viewed as lines of improvement.

160 We thank the reviewer for all his comments and the corresponding improvements that (we believe) resulted in the manuscript. We give a detailed answer to the comments in this review below

165 1. The choice of variables analyzed (sigma's, velocity skewness, ϕ_ϵ , the temperature variance dissipation, and b) have not been justified in an integrated manner. Perhaps the authors meant to state that some of the variables are used to identify whether the flow statistics are in the RSL or not – and some variables are relevant to the stated goal of analyzing VOC measurements using flux-gradient relations and REA. May be structuring the rationale along those lines up-front is worthwhile. That is, the work will be dealing with variables that describe the turbulent Schmidt (and Prandtl) numbers and eddy diffusivity for momentum in the RSL - as well as the similarity in b across scalars (and momentum) in the RSL.

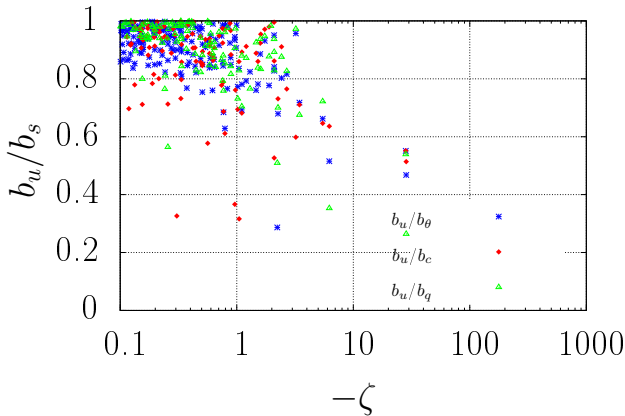
170 We thank the reviewer for the suggestion. It is incorporated in lines 89–95 of the current version of the manuscript

175 2. The linkage between equations (8) and (9) is not entirely clear. The excursions represented by c' are not synonymous to $\bar{c^+} - \bar{c^-}$. I think the authors can do a much better job at justifying the high-order velocity and scalar statistics to b . We agree with the reviewer: the equations for the original Eddy Accumulation method were confusing because we don't apply the EA, and because the Relaxed Eddy Accumulation method equation does not follow from them. Therefore, they were eliminated from the present version: see lines 225–231 of the current version.

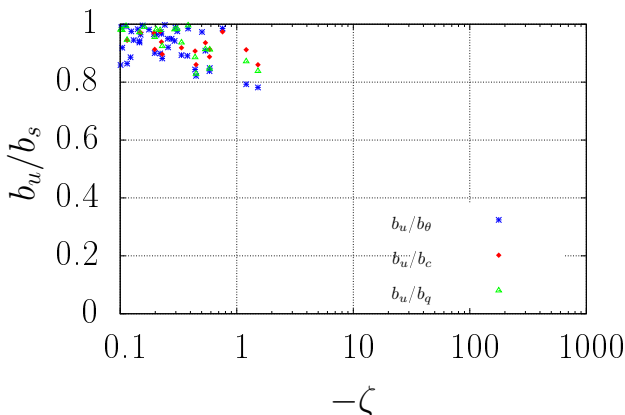
3. A follow-up on comment 2, since this work is all about simulations to determine b , it is worth
180 comparing b for scalars and momentum. Whether b_u/b_s (s is a scalar) is constant for various zenith angles and stability conditions is worth reporting (as b_u may be far more sensitive to the roughness elements here than the sourcesink distribution).

We thank the reviewer for the comment. In this regard, we introduced new results on b_u at the
185 end of section 6, lines 435–450. Overall, there are indications that the zenith angle Z may also influence b_u , but they are not as strong as with b_c , b_θ and b_q . We chose not to present results in terms of b_u/b_s : To keep the paper's narrative cohesive, results are given in terms of b_u , as done with the scalars. However, we do show in the next four figures below the results for b_u/b_s against ζ for the totality of data and for the three zenith-angle classes. We believe that the results incorporated into the manuscript are easier to interpret and deal with the subject to the extent that is possible with the present dataset.

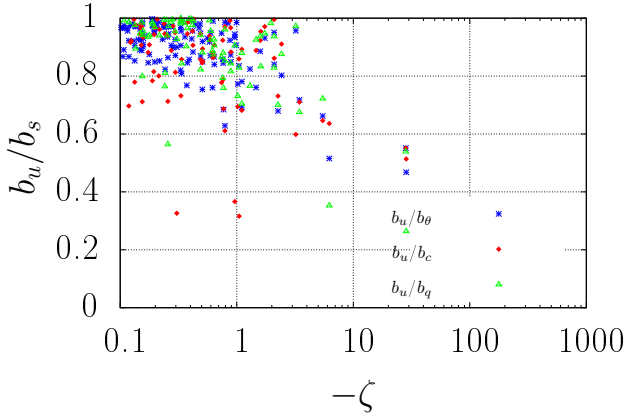
190 all data:



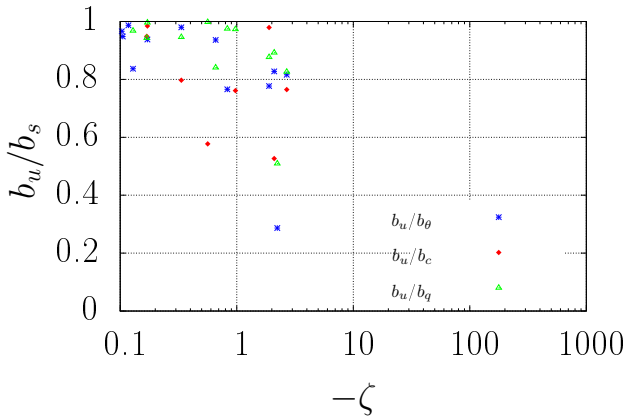
0 < |Z| ≤ 20:



195 20 < |Z| ≤ 60:



$60 < |Z| \leq 90$



4. The equality in coefficients b_s does not necessarily require perfect similarity. For example, for two scalars say s_1 and s_2 , then $R_{w,s_1} \frac{\sigma_{s_1}}{s_1^{+/-} - s_1^{-/-}} = b_{s_1}$, and $R_{w,s_2} \frac{\sigma_{s_2}}{s_2^{+/-} - s_2^{-/-}} = b_{s_2}$. Equating b_{s_1} to b_{s_2} does not necessarily require that $R_{w,s_1} = R_{w,s_2}$ as should be evident from the aforementioned definitions.

The reviewer is of course right, and we admit the oversight. We have changed the text accordingly in lines 246–248.

205 5. Horizontal and vertical velocity skewness values - the flume experiments by Poggi et al. (2004) - figure below suggests that the cross-over height of skewness sign reversal dependence on the vegetation density per se. For dense canopies, the figure below suggests that both skewness values switch signs – and at different levels. This hints that the definition of the RSL thickness will vary with the statistic being analyzed (as expected).

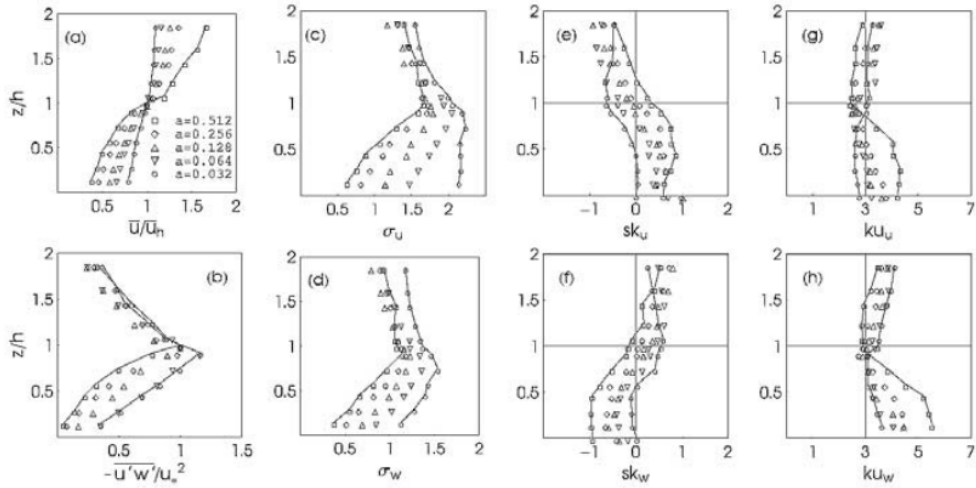


Figure 3. Variation of temporally- and horizontally-averaged moments with normalized height (z/h) for (a) mean longitudinal velocity, (b) mean shear stress, (c) longitudinal velocity standard deviation ($\sigma_u = \overline{u'^2}^{1/2} / u_*$), (d) vertical velocity standard deviation ($\sigma_w = \overline{w'^2}^{1/2} / u_*$), (e-f) longitudinal and vertical velocity skewness ($sk_u = \overline{u'^3} / \sigma_u^3$ and $sk_w = \overline{w'^3} / \sigma_w^3$), and (g-h) longitudinal and vertical velocity kurtosis ($ku_u = \overline{u'^4} / \sigma_u^4$ and $ku_w = \overline{w'^4} / \sigma_w^4$). Solid lines represent the sparsest and densest canopies.

We thank the reviewer for pointing this out. First, we included the new reference in the discussion of Sk_u in the (new) lines 189–192. Then, we included results for the u -skewness in the new Figure 5, and changed the text accordingly in lines 273–283. Overall, the new Sk_u analysis confirms the results previously obtained with Sk_w .

6. The apparent agreement between σ_w/u^* and MOST scaling may be due to self-correlation (see Cava et al., 2008). Certainly, more needs to be done to make a convincing case it is not all about selfcorrelation.

Please see our answer to the same issue in item 1, Reviewer 1, above. Like Caval et al., we did randomize our dataset and like them we concluded that our results do not suffer from suprious correlation.

7. The authors should comment that all the normalized variances are above MOST predictions - but as discussed in Katul et al. (1995), inhomogeneity in the RSL impacts variances (i.e. the variance exceeds what would have predicted by the flux alone) but not necessarily fluxes. So, why is this result significant to VOC measurements – the fluxes may be the same but the variances higher in the RSL? Unless the authors meant to tie this finding to their REA and similarity theories (i.e. to quantities such as $\frac{\sigma_{s1}}{s_1^+ - s_1^-}$.)

We discuss the point further, following the reviewer's suggestion, in lines 331–334. But the crucial point is the following: in this manuscript, we are investigating fruitful approaches to

230 understand the Amazonian RSL a little better, and maybe to better estimate fluxes. It would
take us too far (and out of scope) to actually devise and test methodologies for flux estimation
procedures applicable to substances such as VOCs whose high-frequency measurement is dif-
ficult. Notice that if all we have is a flux-variance behavior with stability of the type shown in
Fig. 4, and if the flux-variance method is the only one available, then the corresponding flux
estimates will suffer from the large scatter in the data. Then, if we now look at Fig. 6 (small
235 zenith angles), the scatter is much less: if the flux-variance method were the only one avail-
able, fluxes estimated for small zenith angles would be more reliable. Of course, this is still
being verified with high-frequency data, but the important fact here (and one that we believe
has not been reported yet) is that there are at least some situations where the difficulties as-
240 sociated with the roughness sublayer could be somewhat alleviated. We found similar results
with the REA, and this is promising, because unlike the flux-variance method it dispenses with
high-frequency measurements. The important point, therefore, is to open up these alternatives
for flux estimates. This is now reinforced in lines 462–467.

8. A corollary comment to point 7 - Why did the authors focus only on the unstable conditions?

245 Stable conditions (i.e. cooling) are equally important to shed light on the de-activation here,
especially for heat and CO₂ (sources and sinks switch signs) may be worth exploring.

We fully agree. Some of our colleagues in the ATTO project (L. Sá and O. Acevedo and
250 collaborators) are exploring stable conditions in depth. On the other hand, most of the mass
transfer (in terms of the time integral of the fluxes) still takes place in daytime conditions, and
we realized that it would be important to contribute to better daytime flux estimates to begin
with. It is also common to analyze stable and unstable conditions separately. In this work,
we decided to focus exclusively (in this current version) on unstable conditions. We hope to
explore this issue from the stable side in the future.

9. Pages 14–15, the role of storage may be significant (see Detto et al., 2010). Also, the authors

255 may want to inspect Figure 7 in Detto et al. (2008).

We thank the reviewer for bringing up this point. We were not aware of Detto et al.'s (2010)
260 results, and they are important to mention. Indeed, it is clear that the results for the storage
term found by Detto et al. (2010) are similar to our results for the zenith angle in the sense
that the storage term is larger at high zenith angles, and that better agreement was found by
Detto et al. for low storage (in the middle of the day, when the zenith angles are lower in
absolute value). We included this discussion in the manuscript in lines 362–369. Unfortunately
we don't have good profiles to test this, and this comparison couldn't be done by us at the
moment. Also, we agree that Detto et al.'s (2008) quadrant analysis would be a powerful tool
for better understanding the causes of scalar dissimilarity in the RSL. However, we believe
265 that this manuscript is already covering a lot of different aspects, so we decided not to include

such analyses at this point. At any rate, an explicit mention to this possibility is given in lines 386–397.

270 10. The conclusions need to present a revised picture of the RSL — does this mean production and dissipation of TKE and temperature variance does not hold — and if so — what does that imply to the usage of K-theory or even the interpretation of constant fluxes with height? More important, the authors should attempt to explore $dF/dz \neq 0$ and its relation to zenith angle? Or $g_\theta(\zeta)$ or χ . This has the most practical consequence of whether fluxes are constant with height or not.

275 The reviewer touches on crucial questions, and it would be an honour to be able to really provide a revised picture of the RSL. At this point, however, we will need to keep to humbler objectives. The reasons are as follows: turbulent budgets need reliable mean profile data, and for this preliminary field campaign we do not have simultaneous good profile data (as already explained above). We also could not find a systematic behavior regarding either TKE or scalar dissipation, as our discussion on g_θ shows. Therefore, we cordially defer more definitive conclusions on the Amazonian RSL for the time when better and more comprehensive data are collected by ATTO.

280

11. References

Detto et al., 2008, Agricultural and Forest Meteorology, 14, 902–916.
285 Detto et al., 2010, Boundary-Layer Meteorology, 136, 407–430.
Cava et al., 2008, Boundary Layer Meteorology, 128, 33–57.
Katul et al., 1995, Boundary Layer Meteorology, 74, 237–260.
Poggi et al. 2004, Boundary-Layer Meteorology, 111, 565–587.

Reviewer: 3

Comments to the Author

290 This is a very important study, well presented by the authors. It has two main qualities: - Usefulness: with the upcoming tall tower in the Amazon, a study of this kind is essential. It will serve as an important reference for future flux analysis at the site; - An important new insight: the finding that zenith angle "controls" the validity of the similarity hypothesis is, to my knowledge, a new one. The reasoning proposed by the authors to explain it makes sense. For these reasons, I recommend 295 publication. I have a few suggestions to the authors, so I am rating it as "accept pending minor revisions"

We thank the reviewer for all his comments and the corresponding improvements that (we believe) resulted in the manuscript. We give a detailed answer to the comments in this review below

300 1. After all screening and filtering for data quality and stationarity, a small percentage of the total data is left for the analysis. Although I understand that this is part of the nature of turbulence

data, I feel it would be important to openly discuss how this fact affects the significance of the results. Do the authors expect that a similar percentage of flux measurements will also need to be discarded at the site? Mabe the authors could mention that when using MOST to infer fluxes from profiles, a larger fraction of data may be used. I also suggest you show (in a table, maybe) what fraction of data is used for each range of zenith angle considered in the analysis. That would hint the reader whether the problems associated with high zenith angle are the same ones that cause lack of stationarity, for instance.

This is an important remark, that we can only answer within the limits of data availability. The percentage of usable data is indeed small, although we should mention that they represent a larger part of the *unstable* runs, on which we concentrated the analysis (this point is now highlighted in the manuscript). Otherwise, we can offer no excuse to the large percentage of data failing quality control, other than report it. This is now explicitly mentioned in lines 156–163.

As regards an analysis of data passing data quality control by zenith angle class, although this certainly would be enlightening, we beg the Reviewer's and Editor's understanding at this point. The way our data analysis programs were written, zenith angle calculations came way after the quality control. We would not have time to reprocess all data before our deadlines. If the Editor thinks this is essential, we will need further time to reprocess all data.

2. In section 3.2, you associate intermittency to skewness. Although I can understand the idea, it sounds strange, because there is another statistical momment, kurtosis, that is inherently associated with intermittency. The same association is later done at line 168.

The reviewer is right, and this is not a paper on intermittency. Our analyses of the skewness played a completely different role, which is that of trying to identify a gradual transition out of the RSL. We found better simply to remove any mention to intermittency, which avoids distracting the reader's attention and misleading him.

3. line 181. The concern about similarity validity depending on the large scales of the flow is certainly a valid one, but it had never been presented before, in the manuscript. Given its importance, I expect that some readers will read the introduction with that idea in mind. I suggest addressing it before.

Done, in lines 99–102

4. Figure 1 is not very informative. How about presenting histograms for each level?

Done.

5. Why arent Sk_u values shown?, given tht they are even included in the discussion that precedes the figure?

335

The u -skewness values are now given: see lines 273–283, and Figure of the current version of the manuscript.

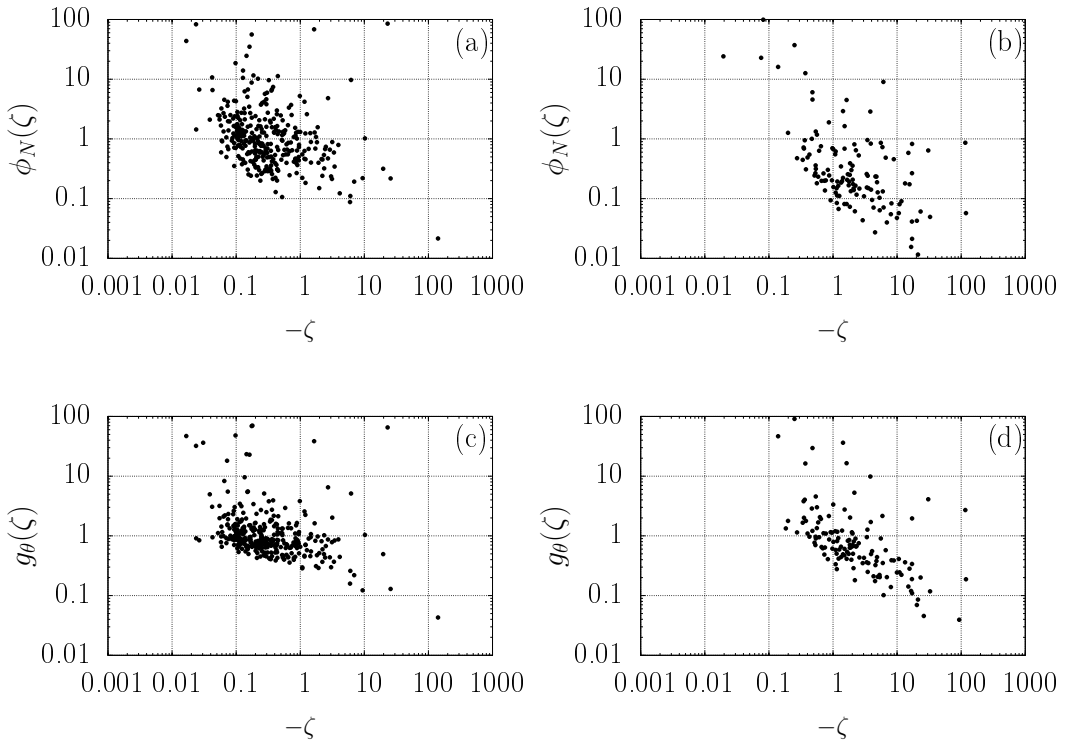
6. Likewise, in figure 3, the dissipation rates (epsilons) could be directly shown as a function of z/L , along with the existent similarity expressions for this relationship. I would be very curious to see that.

340

We did that: we used the classical

$$\phi_N(\zeta) = \frac{\kappa(z-d)N}{u_*\theta_*^2}$$

and compared ϕ_N with g_θ ; the result is shown below.



345

The two pairs of plots are very similar, and the result is understandable: both functions are extracted from the inertial-subrange behavior of the temperature spectrum. Because plotting $\phi_N(\zeta)$ as well clearly does not convey new information, we left g_θ only in the manuscript, in Fig. 3.

350

7. line 329. I like the explanation for the similarity between CO2 and temperature, based on the signs of entrainment. I would also add that the surface fluxes between these two quantities also have opposite signals in the vast majority of the cases.

Done. See 386–386.

8. line 40: remove "to" at the end of the line; line 239: and instead of e

Done.

355 **References**

Andreas, E. L. and Hicks, B. B.: Comments on "Critical test of the validity of Monin-Obukhov Similarity during convective conditions", *J. Atmos. Sci.*, 2002.

Cava, D., Katul, G. G., Sempreviva, A. M., Giostra, U., and Scrimieri, A.: On the Anomalous Behaviour of Scalar Flux-Variance Similarity Functions Within the Canopy Sub-layer of a Dense Alpine Forest, *Boundary-Layer Meteorology*, 128, 33–57, 2008.

Hicks, B. B.: An examination of turbulence statistics in the surface boundary layer, *Boundary-Layer Meteorol.*, 21, 389–402, 1981.

Horst, T. W., Semmer, S. R., and Maclean, G.: Correction of a Non-orthogonal, Three-Component Sonic Anemometer for Flow Distortion by Transducer Shadowing, *Boundary-Layer Meteorology*, 155, 371–395, doi:10.1007/s10546-015-0010-3, <http://dx.doi.org/10.1007/s10546-015-0010-3>, 2015.

Johansson, C., Smedman, A.-S., Högström, U., and Brasseur, J.: Reply, *J. Atmos. Sci.*, 2002.

von Randow, C., Kruijt, B., and Holtlag, A. A. M.: Low-frequency modulation of the atmospheric surface layer over Amazonian rain forest and its implication for similarity relationships, *Agricultural and Forest Meteorology*, 141, 192–207, 2006.

Zahn, E., Chor, T. L., and Dias, N. L.: A simple methodology for quality control of micrometeorological datasets (submitted), *American Journal of Environmental Engineering*, 2016.

Scalar turbulent behavior in the roughness sublayer of an Amazonian forest

Einara Zahn¹, Nelson L. Dias², Alessandro Araújo³, Leonardo Sá⁴,
Matthias Söergel⁷, Ivonne Trebs⁶, Stefan Wolff⁷, and Antônio Manzi⁸

¹Graduate Program in Environmental Engineering (PPGEA), Federal University of Paraná, Curitiba, Brazil

²Department of Environmental Engineering, Federal University of Paraná, Curitiba, PR, Brazil

³Empresa Brasileira de Pesquisa Agropecuária (EMBRAPA), Trav. Dr. Enéas Pinheiro, Belém-PA, CEP 66095-100, Brasil

⁴Centro Regional da Amazônia, Instituto Nacional de Pesquisas Espaciais (INPE), Belém, Pará, Brazil

⁶Luxembourg Institute of Science and Technology, Environmental Research and Innovation (ERIN) Department, L-4422 Belvaux, Luxembourg

⁷Biogeochemistry, Multiphase Chemistry, and Air Chemistry Departments, Max Planck Institute for Chemistry, P.O. Box 3060, 55020, Mainz, Germany

⁸Instituto Nacional de Pesquisas da Amazônia (INPA), Clima e Ambiente (CLIAMB), Av. André Araújo 2936, Manaus-AM, CEP 69083-000, Brazil

Correspondence to: Nelson L. Dias (nldias@ufpr.br)

Abstract. An important current problem in micrometeorology is the characterization of turbulence in the roughness sublayer (RSL), where most of the measurements above tall forests are made. There, scalar turbulent fluctuations display significant departures from the predictions of Monin–Obukhov similarity theory (MOST). In this work, we analyze turbulence data of virtual temperature, carbon dioxide and water vapor in the RSL above an Amazonian Forest (with a canopy height of 40 m), measured at 39.4 and 81.6 m above the ground under unstable conditions. We found that dimensionless statistics related to the rate of dissipation of turbulence kinetic energy (TKE) and the scalar variance display significant departures of MOST as expected, whereas the vertical velocity variance follows MOST much more closely. Much better agreement between the dimensionless statistics with the Obukhov similarity variable, however, was found for the subset of measurements made at low zenith angle Z , in the range $0^\circ < |Z| < 20^\circ$. We conjecture that this improvement is due to the relationship between sunlight incidence and “activation/deactivation” of scalar sinks and fonts vertically distributed in the forest. Finally, we evaluated the relaxation coefficient of Relaxed Eddy Accumulation: it is also affected by zenith angle, with considerable improvement in the range $0^\circ < |Z| < 20^\circ$, and its values fall within the range reported in the literature for the unstable Surface Layer. In general, our results indicate the possibility of better stability-derived flux estimates for low zenith angle ranges.

1 Introduction

In the Atmospheric Surface Layer above the roughness sublayer (RSL) height z_* (approximately 20 three times the height of the roughness obstacles h — Cellier and Brunet 1992), flux estimates based on mean concentration measurements are made with the help of Monin–Obukhov Similarity Theory (MOST) and the corresponding similarity functions. It is now well known, however, that MOST-based similarity functions often fail, to various degrees, in the roughness sublayer. In this region, beyond the classical governing variables found in MOST, there are several more intervening variables, such as tree spacing and vegetation density, among others (Garratt, 1980; Foken et al., 2012; Arnqvist and Bergström, 2015). This is the region where most mean concentration measurements above forests are made, and such is the case with the 82-m tower data analyzed in this work.

In principle, the availability of mean concentration data would make flux-gradient methods a natural choice to estimate scalar fluxes above the forest. Unfortunately, the difficulty of applying 30 MOST in the RSL adds considerable uncertainty to this approach.

Maybe one of the earliest reports of the failure of flux-gradient methods when measurements are performed too close to the roughness elements was made by Thom et al. (1975), who compared flux-gradient and energy-budget Bowen ratio methods over a Pine forest, and found that the dimensionless gradients Φ_M and Φ_H of MOST are underestimated under such conditions. This was generally 35 confirmed by Garratt (1978), who estimated $z_* = 4.5h$ for the momentum flux and $z_* = 3h$ for the sensible heat flux.

In the roughness sublayer, scalar and velocity gradients are weaker than above, leading to higher values of the corresponding turbulent diffusivities (Cellier and Brunet, 1992). Under neutral conditions, the momentum turbulent diffusivity increases by a factor 1.1–1.5, and the sensible heat 40 turbulent diffusivity by 2–3. The turbulent Prandtl number correspondingly decreases from to close to 1 to approximately 0.5 at canopy top (Finnigan, 2000).

Cellier and Brunet (1992) propose a dimensionless factor γ to account for the increase in turbulent diffusivity. Following this suggestion, Schween et al. (1997), using data measured over a 12-m tall oak and pine tree forest, found $\gamma_\theta = 2.2$. They pointed out that the different behavior in the RSL may 45 be due to flux originating below the zero-plane displacement height, since in-canopy air may have significantly different characteristics from above-canopy air. As we will see, zenith angle analyses in the present work give support to this consideration.

Garratt (1980) proposed that for heights $z < z_*$ the vertical gradients depend on an additional length scale z_s , due to the turbulent wake generated by the trees. The author investigated data from a 50 surface covered by scattered trees and shrubs in Australia, referred to as sub-tropical scrub or savannah, of average height 8 m and occupying about 25% of the total surface area. He analyzed data in the range $5 < d/z_0 < 85$ (d is the zero-plane displacement height and z_0 is the surface roughness), suggesting an additional dependence of the dimensionless gradients on the variable z/z_* . Considering the canopy physical characteristics, he found that a relevant length scale is the tree spacing

55 δ , and proposed $z_* = 3\delta$. Regarding Garratt's wake production assumption, it has been argued that this effect dies out rapidly above the canopy and that it is not the main cause for the lack of MOST-compliance in the roughness sublayer (Mölder et al., 1999).

Other attempts to organize roughness sublayer data include the use of z/z_* by Cellier (1986), and Mölder et al. (1999)'s proposal of a function $(z/z_*)^n$ multiplying the dimensionless gradients: 60 Mölder et al. found $n = 1$ for scalars and $n = 0.6$ for momentum; they claim that the use of this factor produces acceptable results. Still, even with this correction, the resulting dimensionless functions in Mölder et al. (1999) display a much larger scatter than what is usually found above the roughness sublayer. Such roughness sublayer "dissimilarity" is not restricted to flux-gradient relationships: the dimensionless standard deviation of a scalar a , σ_a/a_* , has been found to be equally affected (Padro, 65 Katul and Hsieh, 1999; von Randow et al., 2006; Williams et al., 2007; Dias et al., 2009).

In this paper, we analyze roughness-sublayer data collected under the scope of the ATTO project (Amazon Tall Tower Observatory), a German-Brazilian project undertaken under the leadership of Max-Planck-Institute (Germany), Instituto Nacional de Pesquisas da Amazônia (INPA) and Universidade Estadual do Amazonas (UEA) (Brazil). A 325-m tall tower has been erected in a forest 70 site 150 km NE of Manaus, and is currently undergoing instrumentation. Preliminary measurements have been made at an 82-m tall tower built at the site, and some analyses from the measured micrometeorological data are described here.

The main purpose of ATTO is to better understand the role of the Amazonian biome in the context 75 of Global Climatic Changes. Specifically, the project aims at better understanding and modeling of gaseous exchanges between the forest and the atmosphere (Andreae et al., 2015). For many scalars of interest, such as volatile organic compounds (VOCs), the high-frequency measurements needed in the Eddy Covariance Method are still difficult to make (particularly in long-term campaigns), leaving their flux estimates to methods based on the measurement of their mean concentrations and 80 gradients.

Given the importance of correctly estimating trace gas fluxes over the Amazon forest, the lack 85 of a theory for the roughness sublayer is clearly a major obstacle in the understanding of surface-atmosphere interactions with far-ranging implications on the regional and global hydrology, ecology, and climate.

Moreover, given the always present need to take into account site-specific features in any micrometeorological study, we attempt here to provide a general analysis of roughness sublayer-related 90 questions at the ATTO site prior to the construction of the main tower. We expect that once measurements at the main tower become available, a better understanding of the questions preliminarily assessed here will be possible.

The variables analyzed in this study were chosen on the basis of data availability (the preliminary 95 campaigns had to be restricted to fewer variables than those that will be available once ATTO is fully implemented), as well as their usefulness to assess two main questions: (i) how does the Ama-

zonian RSL change the canonical (*i.e.*, measured above the RSL and reported as “classical”) MOST similarity functions, and (ii) how useful/promising would flux-gradient and related methods applied within the Amazonian RSL be for the estimate of the fluxes of VOCs and other chemicals whose
95 high-frequency measurement may be difficult to perform on a long-term basis?

In this work, the sections are organized as follows. In Sect. 2 we describe the experimental site in Amazonian Forest and data measurement; we also show the steps of data quality control. Theoretical concepts used to develop this research are reviewed in Sect. 3, where we describe the dissipation rate, vertical velocity skewness, spectral analysis and relaxed eddy accumulation in light of MOST. An
100 important question of whether the RSL departures from MOST affect the inertial subrange behavior of the scalars is raised here, and an MOST function for the inertial subrange is proposed to address it. In Sect. 4 we discuss these results. Variance method results in the roughness sublayer and the zenith angle influence on several turbulence statistics are shown in Sect. 5, followed by an analysis of scalar similarity indices and their implications for flux estimation in Sect. 6. Finally, in Sect. 7 we
105 make our final considerations.

2 Data measurement and quality control

2.1 Experimental site

The study area is located at Reserva de Desenvolvimento Sustentável Uatumã (RDSU) (Uatumã sustainable development reservation), in the counties of São Sebastião Uatumã and Itapiranga, in the
110 Northeastern of Amazonas state, Brazil. The site is 150 km Northeast of the state capital Manaus, between the coordinates $59^{\circ}10' - 58^{\circ}4'W$ and $2^{\circ}27' - 2^{\circ}4'S$.

In the forest, between 200 and 250 tree species per ha can be found, with a mean height of 40 m and with some individuals reaching 50 m. The site itself is located on a plateau (*terra firme*), with altitude 130 m.

115 The micrometeorological data were measured at an 82-m tower with a rectangular cross section of $2.5 \times 1 \text{ m}^2$ at the site ($2^{\circ}8'40''S$, $59^{\circ}0'10''W$). Micrometeorological instrumentation was installed at the 23, 39.4 and 81.6 m levels (above ground).

In this work, we analyze pilot data from the 39.4 m and 81.6 m heights, measured during April, 2012. The data analyzed are the three wind components u , v and w measured by two sonic anemometers (CSAT3, *Campbell Scientific Inc.* at 39.4 m; R3, *Gill Instruments Ltd.*, at 81.6 m), the sonic temperature (which we assume to be the same as the virtual temperature θ_v), and the mass concentrations (mass of the species/total mass) of CO_2 , c , and H_2O , q , calculated from the corresponding mass densities (mass of the species/volume) measured by two IRGA's (LI-7500A, *LI-COR Inc.*).

120 Both the CSAT3 and the Gill sonics report sonic virtual temperatures. The instantaneous values of θ_v from the sonics and of water vapor density ρ_v and CO_2 density ρ_c from the LI7500 were used to

derive instantaneous values of thermodynamic temperature θ , of specific humidity q and CO₂ mass concentration c . All our results for temperature were calculated with these corrected θ values.

In the same vein, the instantaneous fluctuations of q and c were used to calculate the fluxes and statistics of H₂O and CO₂, without the need of further density corrections (Webb et al., 1980). This is sometimes called “direct method” (Miller et al., 2010; Prytherch, 2011), and produces results comparable to the WPL correction of Webb et al. (1980).

Recently, it has been found that the CSAT3 and Gill R3 sonics may require flow distortion corrections. For CSAT3, these corrections can change, *e.g.*, w' estimates by approximately 8% Frank et al. (2013) and σ_w by approximately 5–6% Frank et al. (2013); Horst et al. (2015). In our case, we tested the flow distortion corrections with the CSAT3 at the 39.4 m height, but our results changed very little: for example, the corrected w' changed by slightly less than 4%. In this work, therefore, the data are processed without the aforementioned flow distortion corrections.

2.2 Quality control

The 10 Hz data were analyzed in 30-min. data blocks (“runs”). Incomplete runs were excluded, and spikes were removed following Vickers and Mahrt (1997). For the next phase of quality control, fluctuations were extracted around a running mean. After that, each run was sub-divided into 15 two-minute subruns, and a local (*i.e.* 2-min.) standard deviation was calculated. Whenever this value was less than a threshold (pre-stipulated based on the sensor accuracy), the whole 30-min. run was excluded.

As a result, 21.5% of the 81.6-m level and 50.2% of the 39.4-m level runs were left. However, after this test, some strongly non-stationary time series remained, mainly in scalar data, even when linear detrending was applied. For this reason, these remaining data were further checked with two tests (both after removal of the linear trend). The first was the Reverse Arrangement Test (Bendat and Piersol 1986, p. 97; Dias et al. 2004), performed on $N = 50$ averages of the 30-min. run and a significance level $\alpha = 0.05$. The second test was defined by us based on a visual scrutiny of the data. It consisted of calculating the difference between the maximum and minimum values of the running mean within each 30 min. run. The run was discarded whenever this difference exceeded $\Delta\theta_v = 1.7^\circ\text{C}$, $\Delta c = 0.11 \text{ g kg}^{-1}$ and $\Delta q = 3 \text{ g kg}^{-1}$. These further tests reduced data availability to 16.8% at the 81.6 m level and 41.5% at the 39.4-m level. For these runs, a 2-D coordinate rotation was applied for the final analyses.

As a percentage of the unstable runs only (which are the ones actually analysed in this work), the figures are 9.4% (81.6 m level) and 24.1% (39.4 m level). Although typical of micrometeorological studies, this somewhat low number of usable runs is bound to limit, for example, the percentage of reliable fluxes that can be retrieved in long-term studies. It is also likely that a larger number of runs fail quality control checks in the RSL in comparison with standard applications of MOST in the Surface Layer. In this work, we needed to concentrate on the analysis of good quality data

at the expense of time coverage. Parallel efforts will be required to increase data availability and representativeness.

3 Theoretical background

165 In this section, we briefly review some results, which are used in the next section to analyze the data.

3.1 Dissipation rate of turbulence kinetic energy

The dimensionless dissipation rate of turbulence kinetic energy (TKE) is given by (Kaimal and Finnigan, 1994)

$$\phi_\epsilon = \frac{\kappa(z-d)\epsilon}{u_*^3}, \quad (1)$$

170 where u_* is the friction velocity, κ is the Von Karman constant and ϵ is the rate of dissipation of TKE. In MOST, a function still widely used to predict ϕ_ϵ is (Kaimal et al., 1972)

$$\phi_\epsilon = (1 + 0.5|\zeta|^{2/3})^{3/2}, \quad -2 \leq \zeta \leq 0, \quad (2)$$

where ζ is the Monin–Obukhov stability parameter. As we shall see, in the roughness sublayer the dissipation rate deviates from the prediction by Eq. (2). In this work, we assess this depart from

175 MOST by extending an index proposed by Mammarella et al. (2008):

$$\chi = \frac{u_*^3/\epsilon}{\kappa(z-d)/\phi_\epsilon} - 1 = \frac{L_\epsilon}{\kappa(z-d)} - 1 \quad (3)$$

In Eq. (1), L_ϵ is the length scale calculated from the friction velocity and the rate of dissipation of TKE, and adjusted to the effect of buoyancy: it can be regarded as an integral scale of the flow.

It can readily be verified that $L_\epsilon/(\kappa(z-d)) = 1 \Rightarrow \chi = 0$ indicates that the dissipation data follow

180 MOST perfectly. Originally, Mammarella et al. (2008) proposed χ to be used only under near-neutral conditions. As our data comprise too few near-neutral runs, it was necessary to take into account stability by including ϕ_ϵ in the denominator of Eq. (1).

3.2 Vertical Velocity Skewness

In the surface layer, the skewnesses of u and w are

$$185 \quad \text{Sk}_w = \frac{\overline{w'^3}}{\sigma_w^3}, \quad (4)$$

$$\text{Sk}_u = \frac{\overline{u'^3}}{\sigma_u^3}. \quad (5)$$

In convective or near-neutral conditions, Sk_w is typically observed to be negative in the roughness sublayer and positive in the inertial sublayer (Raupach and Thom, 1981; Fitzjarrald et al., 1990; von Radow et al., 2006). Some studies suggest that Sk_u tends to be positive in the roughness sublayer

190 and positive/near zero in the inertial sublayer (Kaimal and Finnigan, 1994; Kruijt et al., 2000), but
 there are also indications that it changes sign below or above the canopy height depending on vege-
 tation density Poggi et al. (2004) . At some level above the canopy Sk_w changes sign, and it seems
 reasonable to regard this level to be a measure of the roughness sublayer height. According to Fitz-
 jarrald et al. (1990), the negative Sk_w values above canopies are largely due to the fact that there is
 195 something below the “surface” [sic] in canopy layers, and there can be downward turbulent transport
 of vertical velocity variance associated with the drop in the TKE as one goes into the canopy. Kaimal
 and Finnigan (1994) attribute the considerable scatter in published results primarily to morpholog-
 ical differences between canopies, but at any rate this combination of strongly positive u -skewness
 and strongly negative w -skewness indicates that the turbulence is dominated by downward moving
 200 gusts in the roughness sublayer.

3.3 Scalar dissipation from spectra and inertial subrange behavior

Consider the temperature spectrum in the inertial subrange, in the form

$$k^{5/3} E_{\theta\theta}(k) = \alpha_{\theta\theta} \epsilon^{-1/3} N, \quad (6)$$

where $\alpha_{\theta\theta} = 0.8$, and N is the rate of dissipation of semi-temperature variance (Kaimal and Finnigan, 1994, p. 37).

Also on dimensional grounds, and under the validity of MOST, a similarity function exists that describes the temperature spectrum in the inertial subrange, viz.

$$g_\theta(\zeta) = \frac{\alpha_{\theta\theta} \epsilon^{-1/3} N (z - d)^{2/3}}{\theta_*^2}. \quad (7)$$

Again, we seek to determine to what degree g_θ calculated with roughness sublayer data obeys
 210 MOST scaling. The usefulness of this indicator lies in its limited frequency-range: both ϵ and N are
 inertial-subrange variables in the sense that they are obtained from a straightforward analysis of the
 inertial subrange of the velocity and temperature spectra. Therefore, g_θ is sensitive only to the highest
 range of frequencies (roughly > 0.02 Hz). If the dissimilarity displayed by “bulk” dimensionless
 statistics such as σ_θ/θ_* is due to the larger scales only, then g_θ and similar variables should obey
 215 MOST much more closely than the former. If on the other hand the dissimilarity is spread out through
 all frequency ranges, then g_θ should display the same sort of non-conformance to MOST as the other
 “bulk” statistics.

3.4 The Relaxed Eddy Accumulation method and related analyses

The original Eddy Accumulation method was proposed by Desjardins (1972) with the objective of es-
 220 timating the turbulent flux of chemicals not easily measured at high frequency (see Ren et al., 2011).
 In the method, conditional sampling is performed on the gas, which is directed to either of two
 reservoirs according to the sign and intensity of the vertical wind velocity, w , by means of fast open-
 ing/closing valves. Evident advantages are the fact that the method dispenses with high-frequency

concentration measurements, and that only one-level measurements are needed (Tsai et al., 2012).

225 Still, the method is not without difficulties, and to circumvent them Businger and Oncley (1990) proposed the simpler Relaxed Eddy Accumulation (REA) method, which uses the mean concentrations in each of two conditionally sampled reservoirs, \bar{c}^+ and \bar{c}^- , to calculate the flux as

$$\overline{w'c'} = b_c \sigma_w (\bar{c}^+ - \bar{c}^-), \quad (8)$$

230 where σ_w is the standard deviation of the vertical velocity and b is the relaxation coefficient, that is empirically verified to be a dimensionless constant (it could be a MOST similarity function) of the order of 0.6 (Businger and Oncley, 1990; Katul et al., 1996).

235 Although initially developed and tested for the measurement of CO₂, water vapor and sensible heat fluxes (Pattey et al., 1993; Bash and Miller, 2007), the REA method is often extended for the measurement of other gaseous/scalar fluxes, usually with direct sensible or latent heat fluxes used as proxies to estimate b . For example, Zhu et al. (2000) used it to calculate ammonia fluxes, and Mochizuki et al. (2014) for isoprene and monoterpenes fluxes; Matsuda et al. (2015) used it to estimate sulfate and PM_{2.5} fluxes ; Bowling et al. (1998) used it to calculate isoprene fluxes, Bash and Miller (2007) and Sommar et al. (2013) for mercury fluxes and Moravek et al. (2014) used for peroxyacetyl nitrate fluxes.

240 In the ATTO project, we will be interested in the fluxes of several chemicals whose high-frequency measurement is still too laborious, too expensive, or downright impossible. Among these compounds are the VOCs released by the forests, the monoterpenes and isoprene being the most abundant followed by alcohols, carbonyls, acids, aldehydes, ketones and esters. If applicable, then, the REA method will be an invaluable tool.

245 However, strictly speaking, to be valid the method requires that the same value of b apply to all scalars. A sufficient condition for this to happen, and the simplest — although by no means necessary — is the validity of the well-known hypothesis of perfect similarity between scalars (Hill, 1989; Dias and Brutsaert, 1996), which often fails under unstable conditions due to phenomena originating above the surface layer and to the transport of scalar variance from above (Cancelli et al., 250 2012, 2014). Furthermore, the physics of the roughness sublayer proper may complicate this picture even more.

255 Therefore, before applying the REA method to measurements made close to the canopy over a forest, it is important to assess both the validity of scalar similarity and the equality of the b 's for all scalars. A review of several REA studies by Tsai et al. (2012) showed that b can vary as much as between 0.2 and 0.9, revealing the importance of its correct estimation. In Table 1 we give some values found in the literature outside of the roughness sublayer, and in Table 2 values found by Gao (1995) for the roughness sublayer for different values of the leaf-area index.

Table 1. REA coefficients measured above the roughness sublayer, where z is the measurement height (in meters) and numbers between brackets are the height of the canopies.

Author(s)	Businger and Oncley (1990)	Katul et al. (1996)	Baker et al. (1992)
$z(m)$	4	5	–
Cover	crops	Corn (2.4 m) Grass (0.10 m)	soybean field
b_θ	0.6	0.58 ± 0.11	–
b_q	0.6	0.58 ± 0.15	0.56
b_c	–	0.56 ± 0.06	0.56
b_{O_3}	–	0.56 ± 0.06	–

Table 2. REA coefficients measured within the roughness sublayer (Gao, 1995).

z (m)	43.1	34.2	18	14.4	10.5	5.9
b_θ	0.58 ± 0.04	0.55 ± 0.04	0.51 ± 0.03	–	0.61 ± 0.06	0.62 ± 0.09
b_q	–	0.55 ± 0.02	0.51 ± 0.05	0.61 ± 0.05	–	–

4 Results

4.1 Dissipation rates

260 The rates of dissipation of TKE for each run were calculated from the longitudinal spectra on the basis of Kolmogorov's local isotropy theory (Kolmogorov, 1941). For each run, the inertial subrange was identified and a linear regression with an imposed $-5/3$ slope was calculated to determine ϵ . With ϵ , we calculated ϕ_ϵ in Eq. (1) and the index χ in Eq. (1).

The results can be seen in Fig. 1 where the histograms of χ at two levels are shown. As mentioned 265 before, in the region of validity of MOST, we would expect the χ 's to cluster around 0.

We find that, close to the canopy top, at 39.4 m, the integral scale L_ϵ often far exceeds $\kappa(z - d)$: this means that the latter is not a good estimate of the integral scale, as often found in the roughness sublayer. These results are in agreement with the findings by Rao et al. (1973) e Mammarella et al. (2008). At 81.6 m the spread of χ around zero is somewhat (but not very much) smaller, suggesting 270 that, as expected, we are reaching the upper limit of the roughness sublayer at these heights, again in agreement with what is usually found in the literature.

4.2 Velocity Skewness

In Fig. 2, we show the horizontal and vertical velocity skewness for the levels 39.4 m and 81.6 m, as a function of the stability parameter ζ . The results confirm those found above with the dissipation rate

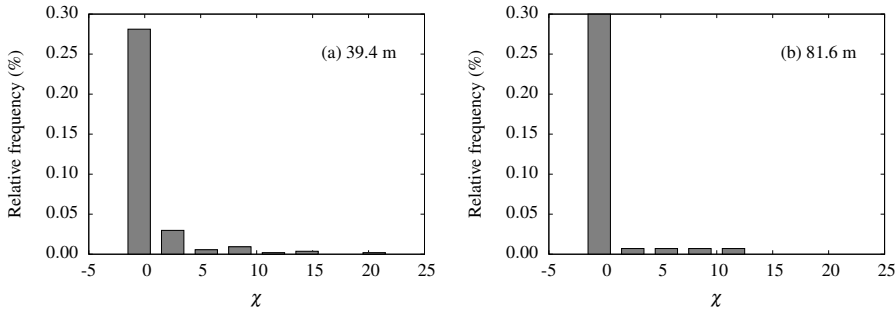


Figure 1. Histograms of χ (see Eq.) at (a) 39.4 and (b) 81.6 cm.

275 in Sect. (4.1): roughness sublayer characteristics are still evident at the upper level, being obviously
 more pronounced at the lower level, where Sk_w reaches close to -0.8 . It is noteworthy that at the
 39.4-m level, in spite of the prevalence of negative values of Sk_w , positive values typically associated
 with the surface layer can also be found. This suggests that the roughness sublayer height is actually
 varying from run to run, or that the physical picture is more complicated, with the possibility of
 280 positive skewnesses inside the roughness layer. The skewness Sk_u of the longitudinal velocity shows
 the opposite behavior, with a predominance of positive values at the 39.4 m level, and a trend towards
 negative values higher up. This confirms, at least partially, the findings of Poggi et al. (2004). Clearly,
 the subject needs further research.

4.3 Inertial subrange similarity

285 Similarly to the analysis of the longitudinal velocity spectra, we identified for each run the inertial
 subrange of the temperature spectrum and fitted a linear regression with a $-5/3$ slope, in order to
 extract the rate of dissipation of semi-variance of temperature, N . From the latter, and ϵ , the value
 of g_θ in Eq. (7) was calculated. It is plotted against ζ for the two levels, in Fig. 3-a and 3-b. There
 is a clear pattern of decreasing g_θ with ζ , but still there is large scatter typical of roughness sublayer
 290 results.

This analysis suggests that inertial-subrange scales, approximately in the range 0.02–0.8 Hz, are
 also influenced by roughness sublayer effects: in other words, restricting the analysis to a range of
 smaller scales does not improve appreciably the predictions of MOST. Similar plots and results were
 also obtained for the other scalars (water vapor and CO_2), but are not shown here.

295 5 Variance method results

5.1 General behavior in the roughness sublayer

The “variance method”, pioneered by Tillman (1972), is widely used in micrometeorology for several purposes, including quality control procedures (Foken and Wichura, 1996; Thomas and Foken,

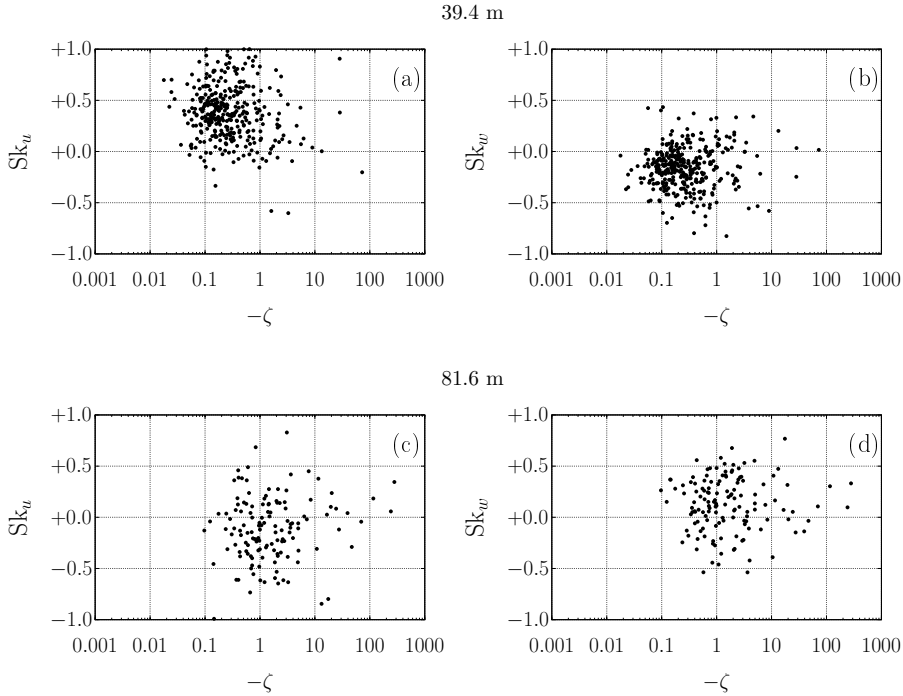


Figure 2. Horizontal (Sk_u) and vertical (Sk_w) velocity Skewness: (a) Sk_u at 39.4 m; (b) Sk_w at 39.4 m ; (c) Sk_u at 81.6 m; and (d) Sk_w at 81.6 m.

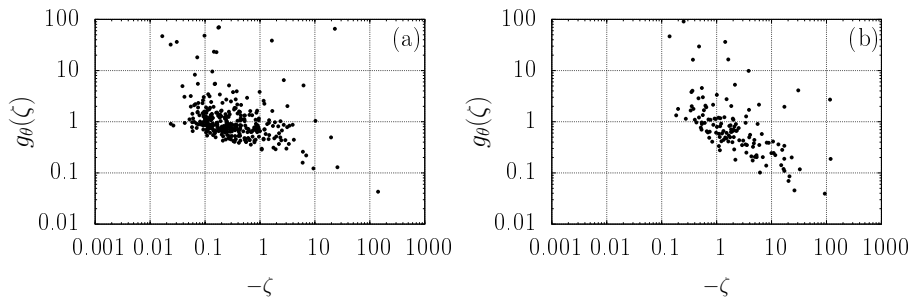


Figure 3. Inertial subrange similarity for temperature spectra: (a) 39.4 m and (b) 81.6 m.

2002; Lee et al., 2004) and flux estimation (Hong et al., 2008). Here, we consider similarity functions of the type $\phi_a = \sigma_a / |a_*|$, where σ_a is the scalar standard deviation, and a_* the scalar's turbulent scale, defined by

$$\overline{w' a'} = u_* a_*, \quad (9)$$

as well as $\phi_w = \sigma_w / u_*$.

In the particular case of ϕ_w in stable conditions, it has been argued that its observed behavior
305 for large ζ may be an artifact of the self-correlation effects raised by Hicks (1981) (see Pahlöw
et al. (2001)). Even though we are dealing with unstable conditions, we applied the randomization
procedure recommended by Andreas and Hicks (2002) to test for possible self-correlation effects.

The randomized ϕ -functions (not shown) tended to follow a $-1/3$ power law in the whole range of
310 observed ζ 's, even at near-neutral conditions, where the original data follow the predicted similarity
functions. Our results are quite similar to those of Cava et al. (2008).

We also calculated the scalar fluxes for fairly to highly unstable conditions ($-\zeta > 0.2$) using the
flux-variance method, and compared them with the measured fluxes. We obtained high correlations
(in fact, higher than those reported by Cava et al. (2008)). As these authors comment, these fluxes
315 are calculated without knowledge of u_* , and the success of the method under these more unstable
conditions gives independent confirmation that spurious correlation is not contaminating our analyses.

Figures 4 and 5 show ϕ_w , ϕ_c , ϕ_q and ϕ_θ for both measurement levels. Only negative CO₂ fluxes
($c_* < 0$) and positive latent and sensible heat fluxes ($q_* > 0$, $\theta_* > 0$) were considered, for unstable
320 conditions $\zeta < 0$. In the figures, we plot empirical $\phi_a(\zeta)$ functions from experimental data for which
good MOST agreement was observed (Katul et al., 1995).

Once more, the large scatter typical of roughness sublayer data is found: notice that the scatter
is much larger in ϕ_θ , ϕ_c and ϕ_q than in ϕ_w . Williams et al. (2007) suggest that this lack of
325 MOST-compliance may be associated with heterogeneity of sources and sinks inside the canopy,
contributing to the larger standard deviation (relative to the scalar turbulent scale).

This tendency of ϕ_a data in the roughness sublayer to lie above the corresponding MOST functions
is generally observed in field experiments (Cava et al., 2008; Dias et al., 2009), but a definitive
explanation for it is still lacking.

The ϕ_w data, on the other hand, show the opposite trend (they fall *below* the corresponding
330 MOST function for the surface sublayer), with much less scatter than in the scalar case.

Notice that this RSL “excess variance” (in comparison with MOST predictions) does not impact the fluxes (Katul et al., 1995); it does however make hypothetical flux estimates with the flux-variance method much more uncertain in the RSL (Dias et al., 2009). In the next section, we show
this can be reduced significantly by taking into account the Zenith angle.

335 5.2 Zenith angle influence

It is known that the zenith angle (Z) can influence transfer characteristics between a vegetated surface and the atmosphere, e.g. the scalar roughness length (Sugita and Brutsaert, 1996). Iwata et al. (2010) note that, above tall vegetation, the vertical distribution of sources and sinks of scalars can vary both seasonally and during the day, depending on how deep light penetrates into the canopy.

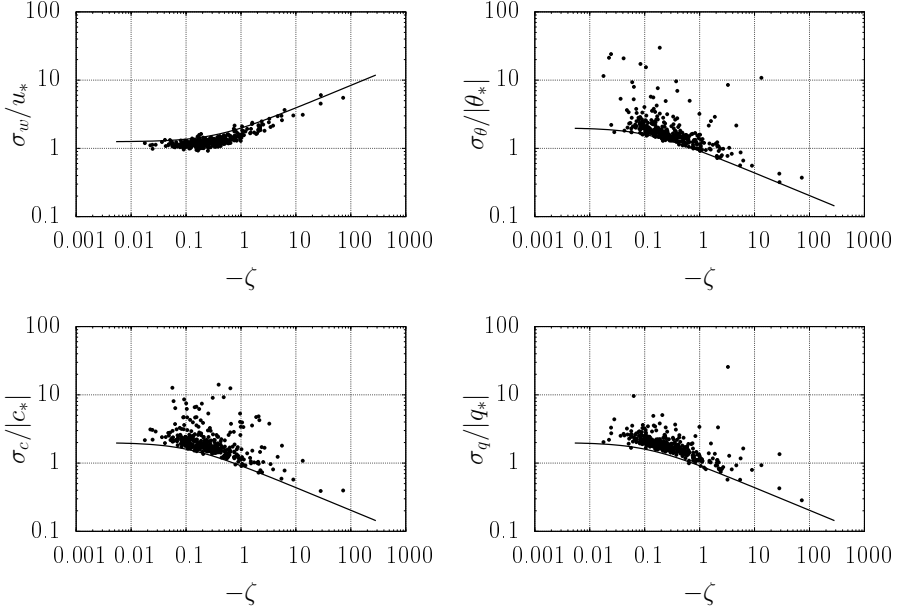


Figure 4. Dimensionless standard deviation for vertical velocity (a), temperature (b), CO₂ (c) and water vapor (d) — 39.4 m.

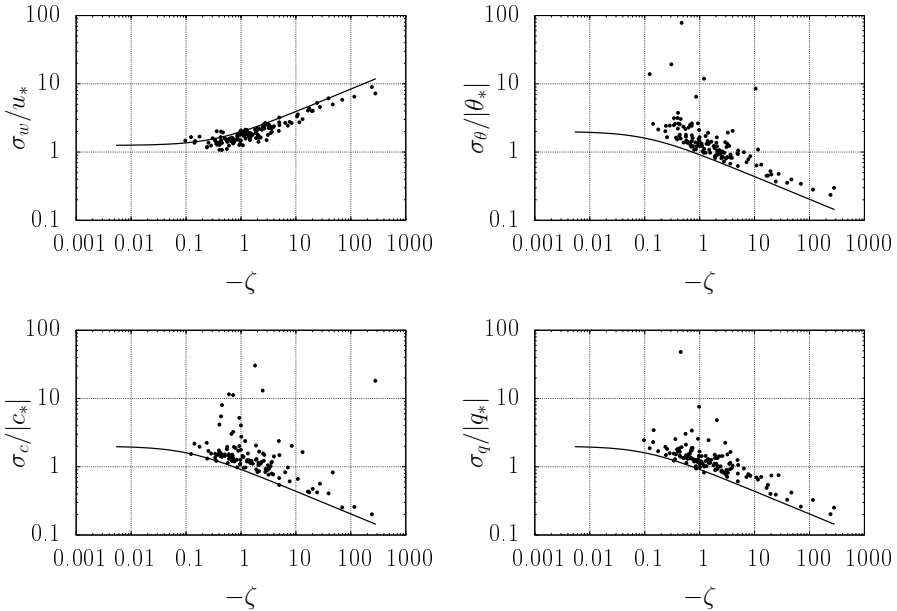


Figure 5. Dimensionless standard deviation for vertical velocity (a), temperature (b), CO₂ (c) and water vapor (d) — 81.6 m.

340 Therefore, the zenith angle is an obvious candidate as a possible effect on scalar transfer between

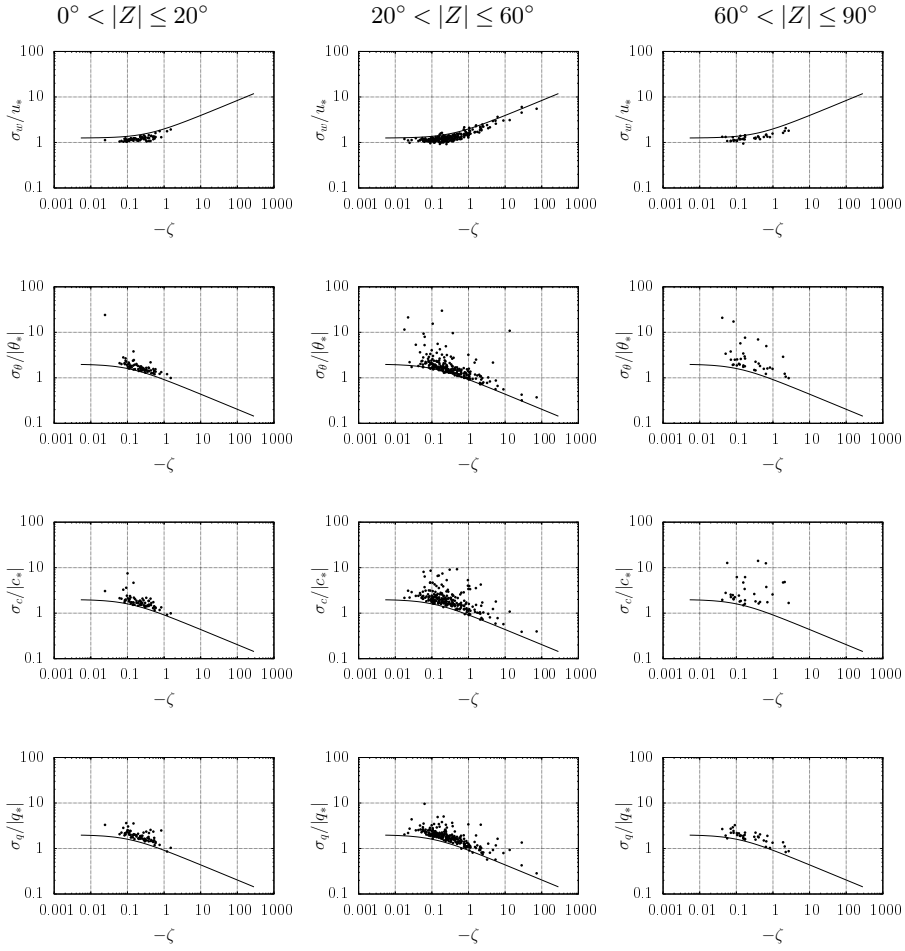


Figure 6. Dimensionless standard deviation with solar angle – 39.4 m. First row shows the velocity similarity function, second shows temperature function and third and fourth show CO₂ and water vapor, respectively.

the canopy and the atmosphere. In the following, we re-do the ϕ_a analysis for three different classes of zenith angle (which were found by trial-and-error to produce best results for the central class): $0^\circ < |Z| \leq 20^\circ$, $20^\circ < |Z| \leq 60^\circ$ and $60^\circ < |Z| \leq 90^\circ$.

In Fig. 6 (for the 39.4-m level), there is considerable improvement in the similarity relationships for all scalars when the sun is high, in the $0^\circ < |Z| \leq 20^\circ$ class of central zenith angles. Results are better for temperature than for CO₂ and H₂O, but this may be related to intrinsic difficulties of measuring the latter: dust and vapor condensation on the IRGA mirror surfaces, and the effects of sensor separation, are possible causes (Tsai et al., 2012). Similar results were found for the 81.6-m level.

These results are encouraging: at least in the hours around noon, similarity relationships as good as those observed in the surface layer over low vegetation can be obtained. This opens up the possibility

of retrieving fluxes, by means of a host of standard MOST methods for these hours of the day. The results also require explanation. It is not immediately clear why these low zenith angles produce best results, but at least two (entirely phenomenological) explanations seem possible. One is vertical
 355 heterogeneity of sources and sinks, such as highlighted by Tsai et al. (2012): obviously, these sources and sinks may be more heterogeneous in the vertical under lower sunlight penetration. Horizontal heterogeneity, on the other hand, may also be playing a role: the vegetation height is not uniform, and a patchwork of shaded regions is clearly visible, from the tower, at higher values of the zenith angle. This may be enough to “activate”/“deactivate” sources of heat, CO₂ and H₂O at the nominal
 360 source level $z - d$, producing what is effectively a non-homogeneous horizontal surface with local advection effects, which may be very hard to identify with standard techniques.

Still with respect to our results for the zenith angle, it is important to mention that similar effects were found by Detto et al. (2010) with regard to the storage term $z \frac{\partial s}{\partial t}$, where s is the scalar’s concentration. They found that for small storage, of the order of 0.5% of the scalar flux, the scatter in the
 365 $\phi_{\theta, q, c, m}$ (where m is for methane) was considerably smaller than under other conditions. Moreover, larger storages were observed around sunset and sunrise (notice that this will correspond to larger (in absolute value) zenith angles). Therefore, there may be a connection between Detto et al. (2010)’s results and ours. Unfortunately, concurrent good mean profile and turbulence data were not available in our dataset, precluding further analyses.

370 6 Scalar similarity indices and implications for flux estimation

6.1 Transport efficiencies

Not surprisingly, it turns out that success or failure of MOST-predictions in the roughness sublayer is also related to the degree of scalar similarity, although it seems that this aspect of RSL turbulence has not yet been fully explored. Two simple indices that are able to describe similarity between the
 375 fluxes of two scalars a and b are:

$$\text{rte}_{ab} = \frac{r_{wa}}{r_{wb}}, \quad (10)$$

$$\text{ste}_{ab} = 1 - \frac{||r_{wa} - r_{wb}||}{|r_{wa}| + |r_{wb}|}, \quad 0 \leq \text{ste}_{ab} \leq 1, \quad (11)$$

where r_{wa} is the correlation coefficient between the vertical velocity fluctuation w' and the scalar fluctuation a' . Different from the correlation coefficient between the two scalars, r_{ab} , rte_{ab} is a better
 380 descriptor of scalar flux similarity (Cancelli et al., 2012). ste_{ab} , proposed by Cancelli et al. (2012), has a similar interpretation, but is explicitly designed so that, unlike rte_{ab} , it is always bounded from above by 1.

Both rte_{ab} and ste_{ab} were calculated for all pairs of scalars. Next, we discuss the results for 39.4 m, shown in Fig. 7, 8 and 9 (the 81.6-m results are similar). Again, we find best scalar similarity for the
 385 $0^\circ < |Z| \leq 20^\circ$ range of zenith angles.

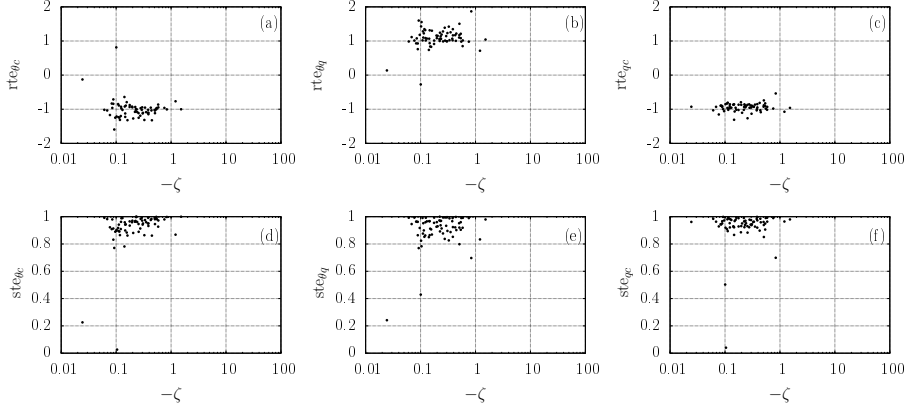


Figure 7. Scalar flux similarity indices rte (above) and ste (below) for $0^\circ < |Z| \leq 20^\circ$; $\theta-c$ (a), (d); $\theta-q$ (b), (e); and $q-c$ (c), (f). For rte, some data points were off the scale.

For most of the runs in the range $0^\circ < |Z| \leq 20^\circ$, ste is between 0.8 and 1.0. The most similar pair of scalar fluxes was CO₂–temperature (c.f. Fig. 7-a and 7-d). We conjecture that this is related to the fact that both scalars have the oposite sign of entrainment fluxes at the top of the atmospheric boundary layer and at the ground; this implies that they are anticorrelated in all the extension 390 of the Atmospheric Boundary Layer (ABL). This is quite common in the unstable ABL. This behaviour is not verified for the H₂O–temperature and CO₂–H₂O pairs: these pairs of scalar fluxes are correlated (H₂O–temperature) and anticorrelated (CO₂–H₂O) at the ground and are anticorrelated (H₂O–temperature) and correlated (CO₂–H₂O) at the top of the ABL. This relationship between entrainment flux and similarity indices was observed, for example, in the LES simulations of 395 Cannelli et al. (2014). However, it is clear that both roughness sublayer and entrainment effects may be impacting scalar similarity, and in that regard more research is needed. For instance, Detto et al. (2008) suggest that these two effects can be discerned by quadrant analysis.

The similarity indices for the other zenith angle intervals are shown in Fig. 8 and 9. In the interval $20^\circ < |Z| \leq 60^\circ$, the scalar fluxes still display a certain degree of similarity. In the interval $60^\circ < 400 |Z| \leq 90^\circ$, however, little similarity is observed. We note that these data often correspond to early morning and late afternoon periods, when scalar sources are usually “deactivated”. These results reinforce the picture of scalar fluxes emanating/being absorbed from different sources/sinks within the canopy and in the soil (c.f. Scanlon and Kustas (2010)).

6.2 Relaxed Eddy Accumulation

405 As reviewed in Sect. 3, the relaxed eddy accumulation is a valuable alternative for the measurement of scalars for which fast-response sensors are not available. This comes at the cost of the extra hypothesis of perfect scalar similarity.

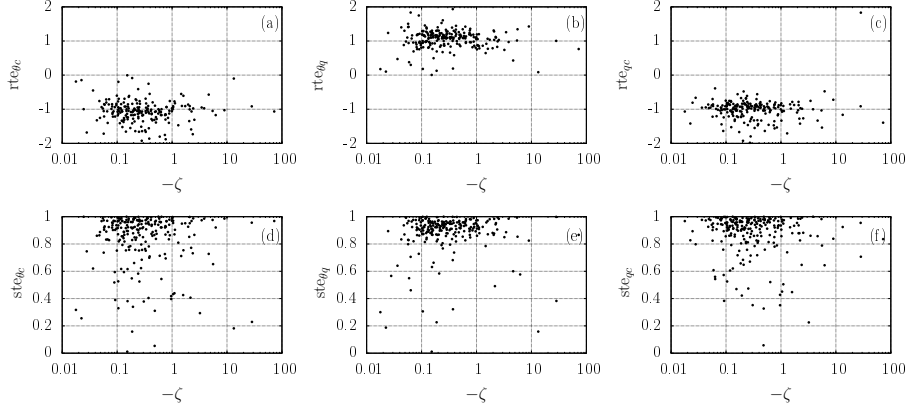


Figure 8. Scalar flux similarity indices rte (above) and ste (below) for $20^\circ < |Z| \leq 60^\circ$; $\theta-c$ (a), (d); $\theta-q$ (b), (e); and $q-c$ (c), (f). For rte, some data points were off the scale.

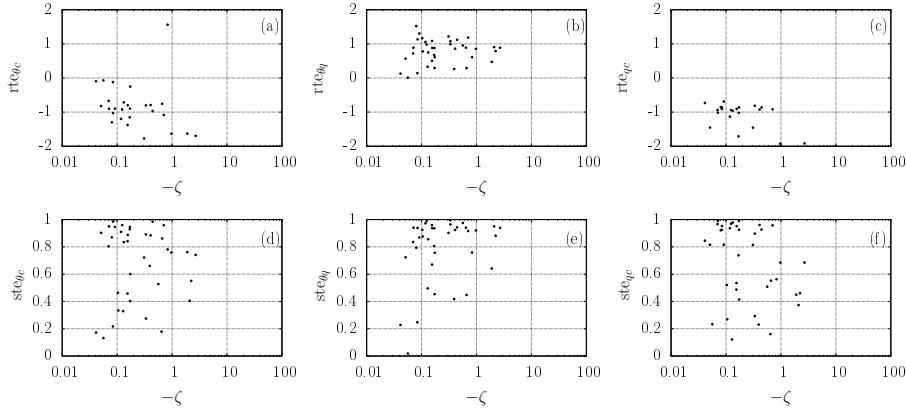


Figure 9. Scalar flux similarity indices rte (above) and ste (below) for $60^\circ < |Z| \leq 90^\circ$; $\theta-c$ (a), (d); $\theta-q$ (b), (e); and $q-c$ (c), (f). For rte, some data points were off the scale.

Since there was no REA system installed at the tower, we have simulated the method using the eddy-covariance data. The fast scalar data were used to obtain updraft and downdraft REA samples 410 by conditional sampling of θ , c and q values for $w > 0$ and $w < 0$, respectively. These simulated samples were then averaged to obtain $\overline{\theta^+}$, $\overline{\theta^-}$, $\overline{c^+}$, $\overline{c^-}$, $\overline{q^+}$ and $\overline{q^-}$.

Given the results found in the previous subsection for rte and ste, it is natural to expect the REA method to perform better, again, in the range $0^\circ < |Z| \leq 20^\circ$. In the following we analyze the relaxation coefficients b defined in Eq. (8), according to scalar and zenith angle.

415 The overall results, not classified according to zenith angle, are shown in Fig. 10, again for unstable conditions only. A few cases for which $b < 0$ were discarded, since the REA, similarly to

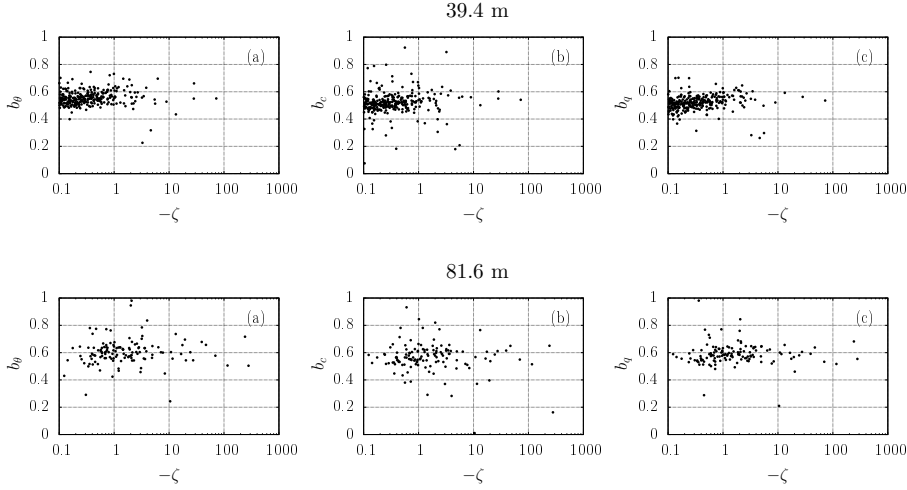


Figure 10. Relaxation coefficient from Eddy Accumulation Method, where (a) and (d) are temperature, (b) and (e) are CO_2 and (c) and (f) are water vapor.

Table 3. Statistics from REA in 39.4 and 81.6 m, where b_θ , b_c and b_q are the relaxation coefficients for temperature, CO_2 and water vapor, respectively.

	39.4 m			81.6 m		
	b_θ	b_c	b_q	b_θ	b_c	b_q
Mean	0.560	0.535	0.522	0.625	0.634	0.593
Median	0.550	0.517	0.519	0.603	0.567	0.584
Standard deviation	0.091	0.158	0.075	0.215	0.710	0.095

flux-gradient methods, cannot cope with counter-gradient fluxes. Our data does not show any significant dependency of b on ζ , in agreement with Katul et al. (1996) and Businger and Oncley (1990).

In table 3, we give the (overall) means, medians and standard deviations of b for each scalar.

420 **All the means are in the same range found by other authors** (e.g. 0.51 – 0.62 by Katul et al. (1996)), which incidentally are values obtained for the surface layer *above* the roughness sublayer. The scatter in our data, however, is larger: at 81.6 m it reaches 0.71 for b_c .

Our mean values of b are also somewhat smaller at 39.4 m (between 0.52 and 0.56) than at 81.6 m (between 0.59 and 0.63). This is similar to the results of Gao (1995) (shown in Table 2), where 425 the mean $b_{\theta,q}$ values are 0.51 next to the canopy top (18 m) and 0.58 in 43.1 m (approximately two times the mean forest height average).

Table 4. Statistics from REA for each zenith angle class

39.4 m				81.6 m		
$0^\circ < Z \leq 20^\circ$	b_θ	b_c	b_q	b_θ	b_c	b_q
Mean	0.555	0.505	0.505	0.613	0.588	0.587
Median	0.546	0.510	0.517	0.622	0.594	0.589
Standard deviation	0.039	0.076	0.047	0.071	0.064	0.091
$20^\circ < Z \leq 60^\circ$	b_θ	b_c	b_q	b_θ	b_c	b_q
Mean	0.558	0.548	0.526	0.632	0.665	0.597
Median	0.551	0.521	0.518	0.596	0.557	0.582
Standard deviation	0.055	0.176	0.084	0.252	0.871	0.087
$60^\circ < Z \leq 90^\circ$	b_θ	b_c	b_q	b_θ	b_c	b_q
Mean	0.591	0.522	0.537	0.731	0.582	0.654
Median	0.546	0.500	0.532	0.772	0.551	0.620
Standard deviation	0.225	0.147	0.044	0.138	0.189	0.094

We classify the b -values according to zenith angle in Table 4. For each zenith angle interval, means and medians are quite similar among the three scalars. Moreover, for most cases in the intervals $0^\circ < |Z| \leq 20^\circ$ and $20^\circ < |Z| \leq 60^\circ$ the standard deviations are larger at 81.6 m.

430 For $0^\circ < |Z| \leq 20^\circ$, the standard deviations of b_θ , b_c and b_q are significantly smaller (by a factor of 2) than for the other two classes, as well as for all data considered together. We note that in general the standard deviations for $60^\circ < |Z| \leq 90^\circ$ are smaller than those for $20^\circ < |Z| \leq 60^\circ$, but they are also more uncertain, due to the small number of points falling into that class. Overall, the better results for small zenith angles are confirmed for the REA method.

435 A version of the REA for momentum is possible. Although it is seldom used to estimate u_* (see Andreas et al. (1998) for such an application), it reads

$$\overline{w'w'} = b_u \sigma_w (\overline{u^+} - \overline{u^-}). \quad (12)$$

To best of our knowledge, the behavior of b_u in the roughness sublayer has not been examined.

440 In table 5 we show the b_u values for the whole data at 39.4 m, as well as for each zenith angle class. As already observed for the scalars, and not shown here, the b_u behavior at 81.6 m is similar, although somewhat more scattered. The b_u behavior mimics that of the scalars in the sense that its means and medians do not vary significantly with the zenith angle, but the scatter (measured by its standard deviation) is much larger for the second class (again the the last class has too few points, which may explain its smaller standard deviation). Therefore, although the zenith angle does not

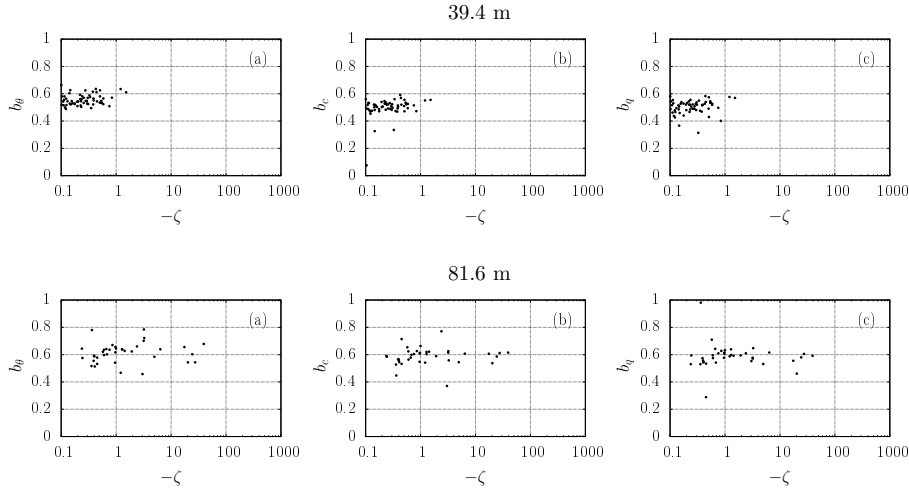


Figure 11. Relaxation coefficient variation with solar angle $-0^\circ < |Z| \leq 20^\circ$. (a) and (d) are temperature, (b) and (e) are CO_2 and (c) and (f) are water vapor.

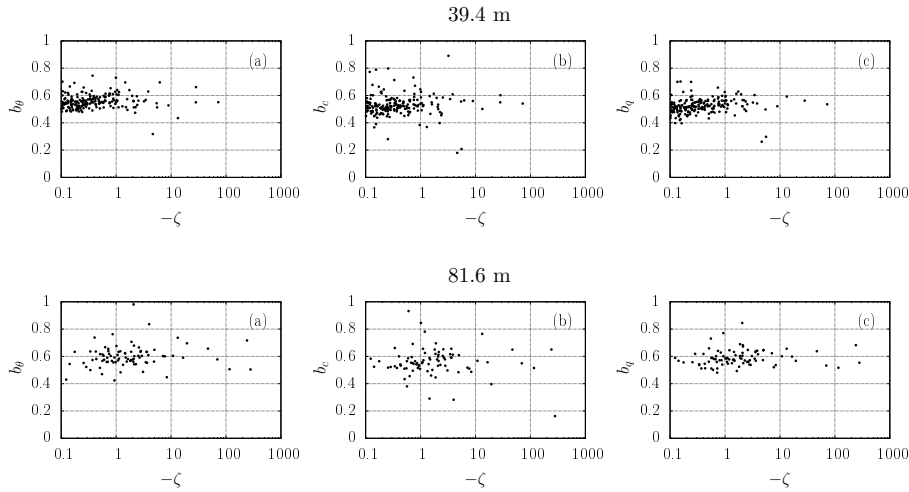


Figure 12. Relaxation coefficient variation with solar angle $-20^\circ < |Z| \leq 60^\circ$. (a) and (d) are temperature, (b) and (e) are CO_2 and (c) and (f) are water vapor. Some data points were off the scale

445 affect the $\phi_w(\zeta)$ function, here, where the mean wind speed \bar{u} is involved, we again detect a signal of Z -dependence.

The plots of b_u against the stability variable ζ and zenith angle classes are shown in Fig. 14. Although in Table 5 it appears that the zenith angle is associated with the increase in scatter, in Fig.

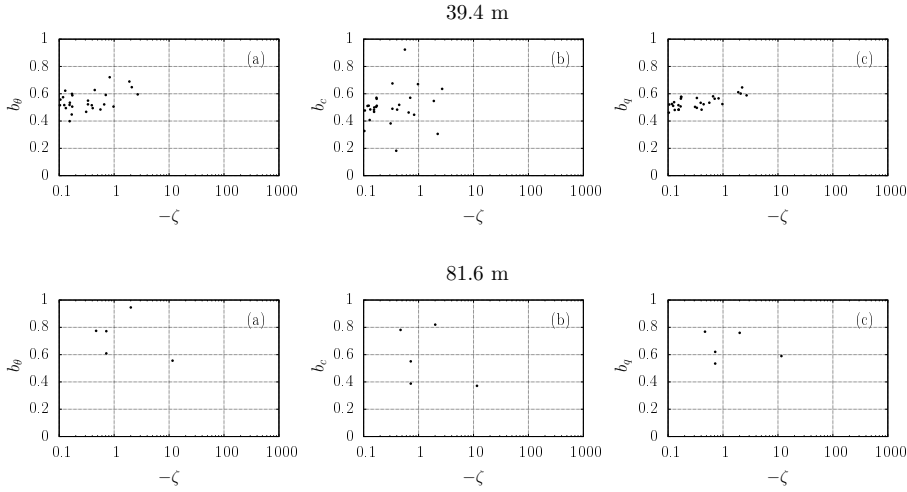


Figure 13. Relaxation coefficient variation with solar angle $-60^\circ < |Z| \leq 90^\circ$. (a) and (d) are temperature, (b) and (e) are CO_2 and (c) and (f) are water vapor. Some data points were off the scale

Table 5. Statistics for b_u (from REA) at 39.4 m.

	all data	$0^\circ < Z \leq 20^\circ$	$20^\circ < Z \leq 60^\circ$	$60^\circ < Z \leq 90^\circ$
Mean	0.544	0.539	0.548	0.539
Median	0.531	0.524	0.531	0.536
Standard deviation	0.178	0.054	0.213	0.053

14 it is also possible that stability may play a role in the scatter as well. Clearly, this issue cannot be
450 completely decided with this dataset, and will require further investigation.

7 Conclusions

An experimental study of the behavior of scalars in the roughness sublayer has been made, with the objective of assessing their departure from the predictions of MOST.

The TKE dissipation rate departures are larger at the 39.4-m level and smaller at the 81.6-m level,
455 suggesting a gradual transition out of the roughness sublayer. This is not confirmed, however, by all turbulence statistics that we analyzed. For example, the dimensionless scalar standard deviations ($\phi_{\theta,q,c}$) at 39.4 and 81.6 do not show significant differences. ϕ_w , on the other hand, remains much closer to the predictions of MOST at the two levels.

Moreover, an analysis of the scalar dissipation rates did not reveal any improvement in scalar be-
460 havior at smaller (i.e. inertial-subrange) scales, indicating that the observed departures from MOST are occurring at all scales.

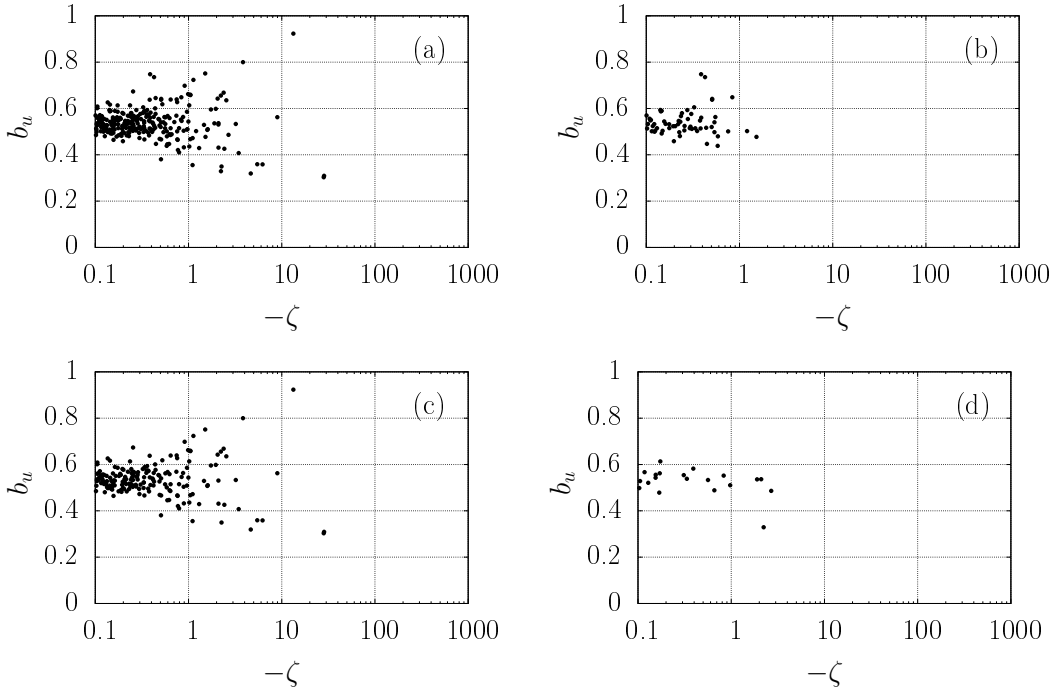


Figure 14. The behavior of b_u at 39.4 m against Obukhov's stability variable ζ and zenith angle Z in the RSL: (a) all data; (b) $0^\circ < |Z| \leq 20^\circ$; (c) $20^\circ < |Z| \leq 60^\circ$; and (d) $60^\circ < |Z| \leq 90^\circ$.

A significant finding in this work is that the degree of departure from MOST predictions is related to the zenith angle. This was found to impact several MOST functions, like $\phi_{\theta,q,c}$, rte, ste and the b coefficient of the REA method, with significant less scatter than what is typically reported in the RSL for small zenith angles. Therefore, exploring these situations could lead to better flux estimates in the RSL. These results are strikingly similar to those found by Detto et al. (2010) with a storage term playing a similar role to Z , and possible links should be revisited in the future.

Fairly good adherence of $\phi_{\theta,q,c}$ to MOST (comparable to what is found in measurements above the RSL) was found for $0^\circ < |Z| \leq 20^\circ$, with increasingly larger scatter as $|Z|$ increases. It is possible that this is related to strongly dissimilar scalar sources and sinks in the vertical when the sun is low, when different physical (*i.e. heating*) and biophysical (*i.e. transpiration and photossynthesis*) forcings are produced throughout the canopy. It is also possible that, at these higher zenithal angles, shading by the irregular tree heights produces a patchwork of different heat (and possibly water vapor and CO_2) sources, adding horizontal inhomogeneity.

The same pattern observed for the dimensionless scalar standard deviations appears with regard to the flux-similarity indices rte and ste. Again, they are closer to the theoretical values of ± 1 and $+1$ (respectively) at lower zenith angles, agreeing with the classical MOST predictions.

Finally, the b coefficients associated with the Relaxed Eddy Accumulation method were also affected by the zenith angle, with considerable improvement in the the range $0^\circ < |Z| \leq 20^\circ$. We
480 confirmed that b does not depend on stability ζ (for unstable conditions), and our values are in the same range as previously observed values. The value of b close to the canopy (39.4 m) may turn out to be slightly lower than above (81.6 m), similarly to what is reported by Gao (1995): a possible variation with height within the RSL needs further research.

Data Availability

485 All data used in this study are kept in the ATTO Database at *Instituto de Pesquisas da Amazônia*. Access should be requested to the ATTO Project Leaders.

Acknowledgements. We thank the Max Planck Society and the Instituto Nacional de Pesquisas da Amazonia for continuous support. We acknowledge the support by the German Federal Ministry of Education and Research (BMBF contract 01LB1001A) and the Brazilian Ministério da Ciência, Tecnologia e Inovação (MCTI/FINEP
490 contract 01.11.01248.00) as well as the Amazon State University (UEA), FAPEAM, LBA/INPA and SDS/CEUC/RDS-Uatumã. Einara Zahn thanks Brazil's CAPES for her Master's scholarship. Leonardo Sá, Antônio Manzi and Nelson L. Dias thank Brazil's National Research & Technology Development Council (CNPq) for their "Productivity in Research" Grants 303728/2010-8, 312431/2013-9 and 303581/2013-1.

References

495 Andreae, M. O., Acevedo, O. C., Araújo, A., Artaxo, P., Barbosa, C. G. G., Barbosa, H. M. J., Brito, J., Carbone, S., Chi, X., Cintra, B. B. L., and et al.: The Amazon Tall Tower Observatory (ATTO) in the remote Amazon Basin: overview of first results from ecosystem ecology, meteorology, trace gas, and aerosol measurements, *Atmospheric Chemistry and Physics Discussions*, 15, 11 599–11 726, doi:10.5194/acpd-15-11599-2015, <http://dx.doi.org/10.5194/acpd-15-11599-2015>, 2015.

500 Andreas, E., Hill, R., Gosz, J., Moore, D., Otto, W., and Sarma, A.: Stability Dependence of the Eddy-Accumulation Coefficients for Momentum and Scalars, *Boundary-Layer Meteorology*, 86, 409–420, doi:10.1023/A:1000625502550, <http://dx.doi.org/10.1023/A%3A1000625502550>, 1998.

Andreas, E. L. and Hicks, B. B.: Comments on “Critical test of the validity of Monin-Obukhov Similarity during convective conditions”, *J. Atmos. Sci.*, 2002.

505 Arnqvist, J. and Bergström, H.: Flux-profile relation with roughness sublayer correction, *Quarterly Journal of the Royal Meteorological Society*, 141, 1191–1197, doi:10.1002/qj.2426, <http://dx.doi.org/10.1002/qj.2426>, 2015.

Baker, J. M., Norman, J. M., and b, W. L. B.: Field-scale application of flux measurement by conditional sampling, *Agricultural and Forest Meteorology*, 62, 31–52, 1992.

510 Bash, J. O. and Miller, D. R.: A Relaxed Eddy Accumulation System for Measuring Surface Fluxes of Total Gaseous Mercury, *Journal of Atmospheric and Oceanic Technology*, 25, 244–257, 2007.

Bendat, J. S. and Piersol, A. G.: *Random Data*, John Wiley & Sons, 2 edn., 1986.

Bowling, D. R., Turnipseed, A. A., Delany, A. C., Baldocchi, D. D., Greenberg, J. P., and Monson, R. K.: The use of relaxed eddy accumulation to measure biosphere-atmosphere exchange of isoprene and other 515 biological trace gases, *Oecologia*, 116, 306–315, 1998.

Businger, J. A. and Oncley, S. P.: Flux Measurement with Conditional Sampling, *Journal of Atmospheric and Oceanic Technology*, 7, 349–352, 1990.

Cancelli, D. M., Dias, N. L., and Chamecki, M.: Dimensionless criteria for the production-dissipation equilibrium of scalar fluctuations and their implications for scalar similarity, *Water Resources Research*, 48, 2012.

520 Cancelli, D. M., Chamecki, M., and Dias, N. L.: A Large-Eddy Simulation Study of Scalar Dissimilarity in the Convective Atmospheric Boundary Layer, *Journal of Atmospheric Sciences*, 71, 3–15, 2014.

Cava, D., Katul, G. G., Sempreviva, A. M., Giostra, U., and Scrimieri, A.: On the Anomalous Behaviour of Scalar Flux-Variance Similarity Functions Within the Canopy Sub-layer of a Dense Alpine Forest, *Boundary-Layer Meteorology*, 128, 33–57, 2008.

525 Cellier, P.: On the validity of flux-gradient relationships above very rough surfaces, *Boundary-Layer Meteorology*, 36, 417–419, 1986.

Cellier, P. and Brunet, Y.: Flux-gradient relationships above tall plant canopies, *Agricultural and Forest Meteorology*, 58, 93–117, 1992.

Desjardins, R. L.: A study of carbon-dioxide and sensible heat fluxes using the eddy correlation technique, 530 Ph.D. thesis, Cornell University, 1972.

Detto, M., Katul, G., Mancini, M., Montaldo, N., and Albertson, J. D.: Surface heterogeneity and its signature in higher-order scalar similarity relationships, *Agricultural and Forest Meteorology*, 148, 902–916, doi:10.1016/j.agrformet.2007.12.008, 2008.

535 Detto, M., Baldocchi, D., and Katul, G. G.: Scaling Properties of Biologically Active Scalar Concentration
 Fluctuations in the Atmospheric Surface Layer over a Managed Peatland, *Boundary-Layer Meteorology*, 136, 407–430, doi:10.1007/s10546-010-9514-z, <http://dx.doi.org/10.1007/s10546-010-9514-z>, 2010.

Dias, N. L. and Brutsaert, W.: Similarity of scalars under stable conditions, *Boundary-Layer Meteorology*, 80, 355–373, 1996.

Dias, N. L., Chamecki, M., Kan, A., and Okawa, C. M. P.: A study of spectra, structure and correlation functions
 540 and their implications for the stationarity of surface-layer turbulence, *Boundary-Layer Meteorology*, 110, 165–189, 2004.

Dias, N. L., Hong, J., Leclerc, M. Y., Nesic, T. A. B. Z., and Krishnan, P.: A Simple Method of Estimating
 Scalar Fluxes Over Forests, *Boundary-Layer Meteorology*, 132, 401–414, 2009.

Finnigan, J.: Turbulence in Plant Canopies, *Annual Review of Fluid Mechanics*, 32, 519–571, 2000.

545 Fitzjarrald, D. R., Moore, K. E., Cabral, O. M. R., Scola, J., Manzi, A. O., and de Abreu Sá, L. D.: Daytime
 Turbulent Exchange Between the Amazon Forest and the Atmosphere, *Journal of Geophysical Research*, 95, 16,825–16,838, 1990.

Foken, T. and Wichura, B.: Tools for quality assessment of surface based flux measurement, *Agricultural and
 Forest Meteorology*, 78, 83–105, 1996.

550 Foken, T., Meixner, F. X., Falge, E., Zetzsch, C., Serafimovich, A., Bargsten, A., Behrendt, T., Biermann, T.,
 Breuninger, C., Dix, S., Gerken, T., Hunner, M., Lehmann-Pape, L., Hens, K., Jocher, G., Kesselmeier,
 J., Luers, J., Mayer, J.-C., Moravek, A., Plake, D., Riederer, M., Rutz, F., Scheibe, M., Siebicke, L.,
 Sorgel, M., Staudt, K., Trebs, I., Tsokankunku, A., Welling, M., Wolff, V., and Zhu, Z.: Coupling pro-
 cesses and exchange of energy and reactive and non-reactive trace gases at a forest site – results of the
 555 EGER experiment, *Atmospheric Chemistry and Physics*, 12, 1923–1950, doi:10.5194/acp-12-1923-2012,
<http://www.atmos-chem-phys.net/12/1923/2012/>, 2012.

Frank, J. M., Massman, W. J., and Ewers, B. E.: Underestimates of sensible heat flux due to vertical velocity
 measurement errors in non-orthogonal sonic anemometers, *Agricultural and Forest Meteorology*, 171–172,
 72–81, doi:10.1016/j.agrformet.2012.11.005, <http://dx.doi.org/10.1016/j.agrformet.2012.11.005>, 2013.

560 Gao, W.: The vertical change of coefficient b, used in the Relaxed Eddy Accumulation method for flux mea-
 surement above and within a forest canopy, *Atmospheric Environment*, 29, 2339–2347, 1995.

Garratt, J. R.: Flux profile relationships above tall vegetation, *Quarterly Journal of the Royal Meteorological
 Society*, 104, 199–211, 1978.

Garratt, J. R.: Surface influence upon vertical profiles in the atmospheric near-surface layer, *Quarterly Journal
 565 of the Royal Meteorological Society*, 106, 803–819, 1980.

Hicks, B. B.: An examination of turbulence statistics in the surface boundary layer, *Boundary-Layer Meteorol.*,
 21, 389–402, 1981.

Hill, R. J.: Implications of Monin-Obukhov Similarity Theory for Scalar Quantities, *Journal of the Atmospheric
 Sciences*, 46, 2236–2244, 1989.

570 Hong, J., Dias, N. L., and Leclerc, M.: Surface-layer scaling for nocturnal turbulence with an evolving low-level
 jet, in: 28th Conference on Agric For Meteorol., American Meteorological Society, Orlando, Fl, 2008.

Horst, T. W., Semmer, S. R., and Maclean, G.: Correction of a Non-orthogonal, Three-Component Sonic Anemometer for Flow Distortion by Transducer Shadowing, *Boundary-Layer Meteorology*, 155, 371–395, doi:10.1007/s10546-015-0010-3, <http://dx.doi.org/10.1007/s10546-015-0010-3>, 2015.

575 Iwata, H., Harazono, Y., and Ueyama, M.: Influence of Source/Sink Distributions on Flux Gradient Relationships in the Roughness Sublayer Over an Open Forest Canopy Under Unstable Conditions, *Boundary-Layer Meteorology*, pp. 391–405, 2010.

Kaimal, J. C. and Finnigan, J. J.: *Atmospheric Boundary Layer Flow*, Oxford University Press, 1994.

580 Kaimal, J. C., Wyngaard, J. C., Izumi, Y., and Coté, O. R.: Spectral characteristics of surface-layer turbulence, *Quarterly Journal of the Royal Meteorological Society*, 98, 563–589, 1972.

Katul, G. G. and Hsieh, C.-I.: A Note on the Flux-Variance Similarity Relationships for Heat and Water Vapour in the Unstable Atmospheric Surface Layer, *Boundary-Layer Meteorology*, 90, 327–338, 1999.

585 Katul, G. G., Goltz, S. M., Hsieh, C.-I., Cheng, Y., Mowry, F., and Sigmon, J.: Estimation of surface heat and momentum fluxes using the flux-variance method above uniform and non-uniform terrain, *Boundary-Layer Meteorology*, 74, 237–260, 1995.

Katul, G. G., Finkelstein, P. L., Clarke, J. F., and Ellestad, T. G.: An Investigation of the Conditional Sampling Method Used to Estimate Fluxes of Active, Reactive, and Passive Scalars, *Journal of Applied Meteorology*, 35, 1835 – 1845, 1996.

Kolmogorov, A. N.: The local structure of turbulence in incompressible viscous fluid for very large Reynolds numbers, *Doklady Akademii Nauk*, 30, 1941.

590 Kruijt, B., Malhi, Y., Lloyd, J., Norbre, A. D., Miranda, A. C., Pereira, M. G. P., Culf, A., and Grace, J.: Turbulence Statistics Above And Within Two Amazon Rain Forest Canopies, *Boundary-Layer Meteorology*, 94, 297–331, doi:10.1023/A:1002401829007, <http://dx.doi.org/10.1023/A:1002401829007>, 2000.

Lee, X., Massman, W., and Law, B.: *Handbook of Micrometeorology*, Kluwer Academic Publishers, 2004.

595 Mammarella, I., Dellwik, E., and Jensen, N. O.: Turbulence spectra, shear stress and turbulent kinetic energy budgets above two beech forest sites in Denmark, *Tellus*, pp. 179–187, 2008.

Matsuda, K., Watanabe, I., Mizukami, K., Ban, S., and Takahashi, A.: Dry deposition of PM2.5 sulfate above a hilly forest using relaxed eddy accumulation, *Atmospheric Environment*, 107, 255 – 261, 2015.

600 Miller, S. D., Marandino, C., and Saltzman, E. S.: Ship-based measurement of air-sea CO₂ exchange by eddy covariance, *Journal of Geophysical Research: Atmospheres*, 115, n/a–n/a, doi:10.1029/2009JD012193, <http://dx.doi.org/10.1029/2009JD012193>, d02304, 2010.

Mochizuki, T., Tani, A., Takahashi, Y., Saigusa, N., and Ueyama, M.: Long-term measurement of terpenoid flux above a *Larix kaempferi* forest using a relaxed eddy accumulation method, *Atmospheric Environment*, 83, 53 – 61, 2014.

605 Mölder, M., Grelle, A., Lindroth, A., and Halldin, S.: Flux-profile relationships over a boreal forest – roughness sublayer corrections, *Agricultural and Forest Meteorology*, 98–98, 645–658, 1999.

Moravek, A., Foken, T., and Trebs, I.: Application of a GC-ECD for measurements of biosphere-atmosphere exchange fluxes of peroxyacetyl nitrate using the relaxed eddy accumulation and gradient method, *Atmospheric Measurement Techniques*, 7, 2097–2119, doi:10.5194/amt-7-2097-2014, <http://www.atmos-meas-tech.net/7/2097/2014/>, 2014.

Padro, J.: An investigation of flux-variance methods and universal functions applied to three land-use types in unstable conditions, *Boundary-Layer Meteorology*, 66, 413–425, 1993.

Pahlow, M., Parlange, M. B., and Porté-Agel, F.: On Monin-Obukhov similarity in the stable atmospheric boundary layer, *Boundary-Layer Meteorol.*, 99, 225–248, 2001.

615 Pattey, E., Desjardins, R., and Rochette, P.: Accuracy of the relaxed eddy-accumulation technique, evaluated using CO₂ flux measurements, *Boundary-Layer Meteorology*, 66, 341–355, 1993.

Poggi, D., Porporato, A., Ridolfi, L., Albertson, J. D., and Katul, G. G.: The effect of vegetation density on canopy sub-layer turbulence, *Boundary-Layer Meteorol.*, 111, 565–587, 2004.

Prytherch, J.: Measurement and parameterisation of the air-sea CO₂ flux in high winds, Ph.D. thesis, University 620 of Southampton, School of Ocean and Earth Science, 2011.

Rao, K. S., Wyngaard, J. C., and Coté, O. R.: The Structure of the Two-Dimensional Internal Boundary Layer over a Sudden Change of Surface Roughness, *Journal of Atmospheric Sciences*, 31, 738–746, 1973.

Raupach, M. R. and Thom, A. S.: Turbulence in and above plant canopies, *Annual Review of Fluid Mechanics*, 13, 97–129, 1981.

625 Ren, X., Sanders, J. E., Rajendran, A., Weber, R. J., Goldstein, A. H., Pusede, S. E., Browne, E. C., Min, K. E., and Cohen, R. C.: A Relaxed Eddy Accumulation system for measuring vertical fluxes of nitrous acid, *Atmospheric M*, 4, 2093–2103, 2011.

Scanlon, T. M. and Kustas, W. P.: Partitioning carbon dioxide and water vapor fluxes using correlation analysis, *Agricultural and Forest Meteorology*, pp. 89–99, doi:10.1016/j.agrformet.2009.09.005, 2010.

630 Schween, J. H., Zelger, M., Wichura, B., Foken, T., and Dlugi, R.: Profiles and Fluxes of Micrometeorological Parameters Above and Within the Mediterranean Forest at Castelporziano, *Atmospheric Environment*, 31, 185–198, 1997.

Sommar, J., Zhu, W., Shang, L., Feng, X., and Lin, C.-J.: A whole-air relaxed eddy accumulation measurement system for sampling vertical vapour exchange of elemental mercury, *Tellus B*, 65, 2013.

635 Sugita, M. and Brutsaert, W.: Optimal Measurement Strategy for Surface Temperature to Determine Sensible Heat Flux From Anisothermal Vegetation, *Water Resources Research*, 32, 2129–3134, 1996.

Thom, A. S., Stewart, J. B., Oliver, H. R., and Gash, J. H. C.: Comparison of aerodynamic and energy budget estimates of fluxes over a pine forest, *Quarterly Journal of the Royal Meteorological Society*, 101, 93–105, 1975.

640 Thomas, C. and Foken, T.: Re-evaluation of integral turbulence characteristics and their parameterizations, in: 15th conference on turbulence and Boundary Layers., American Meteorological Society, 2002.

Tillman, J. E.: The indirect determination of stability, heat and momentum fluxes in the atmospheric boundary layer from simple scalar variables during dry unstable conditions, *Journal of Applied Meteorology*, 11, 783–792, 1972.

645 Tsai, J. L., Tsuang, B. J., Kuo, P. H., Tu, C. Y., Chen, C. L., Hsueh, M. T., Lee, C. S., Yao, M. H., and Hsueh, M. L.: Evaluation of the relaxed eddy accumulation coefficient at various wetland ecosystems, *Atmospheric Environment*, 60, 336–347, 2012.

Vickers, D. and Mahrt, L.: Quality control and flux sampling problems for tower and aircraft data, *Journal of Atmospheric and Oceanic Technology*, 14, 512–526, 1997.

650 von Randow, C., Kruijt, B., and Holtslag, A. A. M.: Low-frequency modulation of the atmospheric surface layer over Amazonian rain forest and its implication for similarity relationships, *Agricultural and Forest Meteorology*, 141, 192–207, 2006.

Webb, E. K., Pearman, G. I., and Leuning, R.: Correction of flux measurements for density effects due to heat and water vapor transfer, *Q J Roy Meteorol Soc*, 106, 85–100, 1980.

655 Williams, C. A., Scanlon, T. M., and Albertson, J. D.: Influence of surface heterogeneity on scalar dissimilarity in the roughness sublayer, *Boundary-Layer Meteorology*, 122, 149–165, 2007.

Zhu, T., Pattey, E., and Desjardins, R.: Relaxed Eddy-Accumulation Technique for Measuring Ammonia Volatilization, *Environmental Science Technology*, 34, 199–203, 2000.